Calculation of quasidegenerate energy levels of two-electron ions

O. Yu. Andreev,[1] L. N. Labzowsky,[1,2] G. Plunien,[3] and G. Soff[3]
[1]*V. A. Fock Institute of Physics, St. Petersburg State University, Ulyanovskaya 1, 198504, Petrodvorets, St. Petersburg, Russia*
[2]*Petersburg Nuclear Physics Institute, 188300, Gatchina, St. Petersburg, Russia*
[3]*Institut für Theoretische Physik, Technische Universität Dresden, Mommsenstraβe 13, D-01062, Dresden, Germany*
(Received 16 December 2003; published 8 June 2004)

Accurate QED calculations of the interelectron interaction corrections for the $(1s2p)2^1P_1$ and $(1s2p)2^3P_1$ two-electron configurations for ions with nuclear charge numbers $10 \leqslant Z \leqslant 92$ are performed within the line profile approach. Total energies of these configurations are evaluated. Employing the fully relativistic treatment based on the $j-j$ coupling scheme these energy levels become quasidegenerate in the region $Z \leqslant 40$. To treat such states within the framework of QED we utilize the line profile approach. The calculations are performed within the Coulomb gauge.

DOI: 10.1103/PhysRevA.69.062505 PACS number(s): 31.30.Jv, 31.10.+z

I. INTRODUCTION

To provide accurate quantum-electrodynamical (QED) evaluations of energy levels for two- and three-electron configurations of highly charged ions (HCI's) has become now an urgent problem in atomic physics. This can be explained by the growing number of experimental data and the necessity to use the energy levels for the evaluation of important characteristics of HCI's, such as, e.g., transition probabilities and recombination cross sections.

In the past an approximate relativistic approach based on variational nonrelativistic wave functions has been used for evaluating energy levels [1]. Numerous theoretical results for few-electron ions have been obtained within the framework of fully relativistic many-body perturbation theory (RMBPT) and relativistic all-order (AO) many-body theory [2]. However, rigorous QED results, which allow for a consequent order-by-order improvement of the accuracy of the calculations have become more and more desirable.

The approximation of noninteracting electrons is commonly employed as a zeroth-order approximation in QED perturbation theory for HCI's in the absence of a quasidegeneracy of levels. Accordingly, within the zeroth-order approximation the energy of the few-electron configuration appears as the sum of the Dirac eigenvalues for the occupied one-electron states. One-electron corrections (termed here as a generalized Lamb shift) include QED radiative corrections, such as the electron self-energy (SE) and vacuum polarization (VP) as well as nuclear corrections—i.e., nuclear size (NS), nuclear recoil (NR), and nuclear polarization (NP), respectively. A few years ago a status report of one-electron energy corrections was presented in detail in [3]. Since then, considerable progress concerning the evaluation of higher-order self-energy corrections has been made [4].

The dominant two-electron contribution is due to the interelectron interaction. *Ab initio* QED results for the first-order interelectron interaction in two-electron ions are known from Ref. [5] (see also [6]). The higher-order corrections are much more intricate. Complete QED calculations of the second-order interelectron interaction have been accomplished for the ground state and for nondegenerate low-lying excited states of He-like and Li-like ions [7–13].

The other important two-electron corrections are the screened self-energy and vacuum-polarization corrections, which have been evaluated in [14–17] for nondegenerate two- and three-electron configurations in HCI's.

Various general bound-state QED approaches have been employed for the derivation of the energy corrections in HCI's. The one most commonly used is the adiabatic *S*-matrix approach, developed by Gell-Mann and Low [18], generalized by Sucher [19] and first applied to bound-state QED corrections in Ref. [20] (see also [5]). The other one is the Green's function approach, first developed in [21] and now applied frequently in a more sophisticated form of the two-time Green's function method [22–24]. Finally, the line profile approach (LPA) is utilized for the same purpose [25,26]. In our previous studies of the QED theory of interelectron interaction in HCI [11,13] this approach has been applied.

In this paper we generalize the line profile approach to the case of quasidegenerate electronic states in two-electron HCI. This problem arises when a complete QED treatment including the relativistic $j-j$ coupling scheme is applied to the fine-structure multiplets of systems with intermediate nuclear charge numbers Z. Some components of the multiplet with equal relativistic quantum numbers turn out to be close enough to each other [the $(1s2p)2\ ^1P_1$ and $(1s2p)2\ ^3P_1$ levels are the standard example].

Up to now the QED theory of the quasidegenerate levels was considered only within the two-time Green's function method for the self-energy screening corrections (without any numerical applications) [27], for vacuum-polarization screening corrections [15], and within the covariant evolution-operator procedure [28] for the second-order interelectron interaction. Numerical calculations for two-electron ions with $Z=10,18$ [28] are so far the only example where bound-state QED has been applied to the evaluation of the energy of quasidegenerate levels taking into account the interelectron interaction up to second order.

In this work we present an extension of the line profile approach which is suitable for the evaluation of energies of any number of the nondegenerate or quasidegenerate levels. The interelectron interaction corrections up to first and sec-

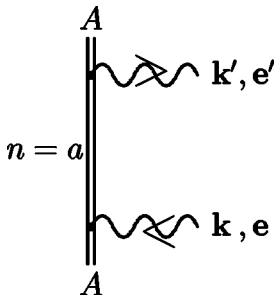

FIG. 1. The lowest-order amplitude of the photon scattering on the atomic electron within the resonance approximation. The double solid line corresponds to bound electrons in the field of the nucleus. The wavy lines with arrows denote the absorption or the emission of a photon with momentum **k** and polarization **e**.

ond order of QED perturbation theory are evaluated for the $(1s2p)2\ ^1P_1$ and $(1s2p)2\ ^3P_1$ levels in a wide range of Z values.

II. LINE PROFILE APPROACH

The problem of the natural line profile in atomic physics was considered first in terms of quantum mechanics by Weisskopf and Wigner [29]. In terms of modern QED it was first formulated for one-electron atoms by Low [30]. In [30] the appearance of the Lorentz profile in the resonance approximation within the framework of QED was described and nonresonant corrections were estimated. Later the line profile QED theory was modified also for two-electron atoms [31] (see also [6,32]) and applied to the theory of overlapping resonances in two-electron HCI's [33,34]. Another application was devoted to the theory of nonresonant corrections [35,36].

It was found in [25] that the LPA provides a convenient tool for calculating energy corrections. Moreover, it clearly determines the limit up to which the concept of the energy of the excited states has a physical meaning—that is, the resonance approximation. The exact theoretical values for the energy of the excited states defined by the poles in the Green's function can be directly compared with measurable quantities only within the resonance approximation, where the line profile is described by the two parameters: energy E and width Γ. Beyond this approximation the evaluation of E and Γ should be replaced by the evaluation of the line profile for the particular process. Moreover, in the case of two-electron atoms the line profile approach was found to be very efficient for the evaluation of the reference-state correction (reducible part of Feynman graphs) for two-electron atoms [37].

A. Line profile approach for one-electron ions

Consider the simplest process of photon scattering on a one-electron ion which is assumed to be in its ground state A (Fig. 1). Using the standard Feynman rules for bound-electron QED [6] yields the expression for the S-matrix element:

$$S_A^{(2)} = (-ie)^2 \int d^4x_u d^4x_d \bar{\psi}_A(x_u)\gamma^{\mu_u} S(x_u,x_d)\gamma^{\mu_d}\psi_A(x_d) \times A_{\mu_u}^{*(k',\lambda')}(x_u) A_{\mu_d}^{(k,\lambda)}(x_d), \quad (1)$$

where $\psi_A(x)=\psi_A(\mathbf{r})e^{-i\varepsilon_A t}$ is the wave function of the electron in the ground state and γ^μ is the Dirac matrix together with the electron propagator

$$S(x_1,x_2) = \frac{i}{2\pi}\int_{-\infty}^{\infty} d\omega\ e^{-i\omega(t_1-t_2)} \sum_n \frac{\psi_n(\mathbf{r}_1)\bar{\psi}_n(\mathbf{r}_2)}{\omega-\varepsilon_n(1-i0)}. \quad (2)$$

Here $A_\mu^{(k,\lambda)}(x)$ denotes the vector potential of the electromagnetic field (photon wave function). The notations $x_u=(t_u,\mathbf{r}_u)$ and $x_d=(t_d,\mathbf{r}_d)$ indicate "up" and "down" vertex coordinates, respectively.

Insertion of the expressions for the electron propagator and the photon wave function yields

$$S_A^{(2)} = (-ie)^2 \int dt_u d^3\mathbf{r}_u dt_d d^3\mathbf{r}_d d\omega_n [\bar{\psi}_A(\mathbf{r}_u)\gamma^{\mu_u} A_{\mu_u}^{*(k',\lambda')}(\mathbf{r}_u)] \times e^{it_u(\varepsilon_A+\omega')} e^{-i\omega_n(t_u-t_d)} \frac{i}{2\pi}\sum_n \frac{\psi_n(\mathbf{r}_u)\bar{\psi}_n(\mathbf{r}_d)}{\omega_n-\varepsilon_n(1-i0)} e^{-it_d(\varepsilon_A+\omega)} \times [\gamma^{\mu_d} A_{\mu_d}^{(k,\lambda)}(\mathbf{r}_d)\psi_A(\mathbf{r}_d)]. \quad (3)$$

Here $\omega=|\mathbf{k}|$ and $\omega'=|\mathbf{k}'|$ are frequencies of the absorbed and emitted photons, respectively, $\mathbf{k},\mathbf{k}'$ are the photon momenta and λ,λ' denote the photon polarizations. The summation over n is extended over the entire Dirac spectrum of electrons in the nuclear Coulomb field, and ε_n are the Dirac energy eigenvalues. Integrating over time variables (t_u,t_d) and abbreviating the expressions in the square brackets by $\bar{\Phi}_A(\mathbf{r}_u)$ and $\Phi_A(\mathbf{r}_d)$, respectively, we can write

$$S_A^{(2)} = (-ie)^2(2\pi)^2 \int d^3\mathbf{r}_u d^3\mathbf{r}_d d\omega_n \bar{\Phi}_A(\mathbf{r}_u) \times \delta(\omega_n-\varepsilon_A-\omega')\frac{i}{2\pi}\sum_n \frac{\psi_n(\mathbf{r}_u)\bar{\psi}_n(\mathbf{r}_d)}{\omega_n-\varepsilon_n(1-i0)} \times \delta(\varepsilon_A+\omega-\omega_n)\Phi_A(\mathbf{r}_d). \quad (4)$$

The function $\Phi_A(\mathbf{r})$ can be considered as a vertex function, which describes the absorption of a photon by an electron in its ground state. Below, we will formulate the resonance approximation, where we can define the energy and width of the level which have a general meaning independent of the features of the considered scattering process. Hence, the energy and width will not depend on the function $\Phi_A(\mathbf{r})$ and thus we may consider the function $\Phi_A(\mathbf{r})$ as arbitrary. In particular, it can account for the interaction with the free electromagnetic field (radiative corrections).

Let us introduce in Eq. (4) the matrix

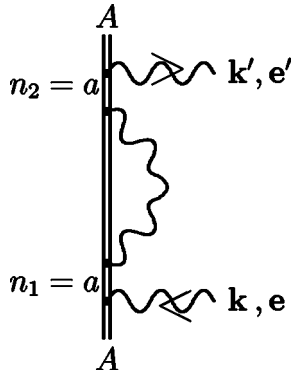

FIG. 2. First-order self-energy insertion into the photon-scattering graph within the resonance approximation.

$$T_{nA} = (-e)\int d^3\mathbf{r}\,\bar{\psi}_n(\mathbf{r})\Phi_A(\mathbf{r}) \tag{5}$$

and integrate over the frequency ω_n. Employing the definition of the transition amplitude U via

$$S = -2\pi i\,\delta(\omega-\omega')U, \tag{6}$$

we derive the expression for the amplitude:

$$U_A^{(2)} = \sum_n \frac{T_{An}^* T_{nA}}{\omega-\varepsilon_n+\varepsilon_A}. \tag{7}$$

We will consider the resonance case when the frequency ω is close to the value $\omega^{\rm res}=\varepsilon_a-\varepsilon_A+O(\alpha)$, where a labels one of the exited states of an ion. In the resonance approximation we have to retain in Eq. (7) only the dominant term with $n=a$ in the sum over n—i.e.,

$$U_{Aa}^{(2)} = \frac{T_{Aa}^* T_{aA}}{\omega-\varepsilon_a+\varepsilon_A} = T^* D^{-1} T. \tag{8}$$

In order to simplify the application of the line profile approach to the many-electron ions we introduce the abbreviated notations

$$T = T_{aA}, \tag{9}$$

$$D = \omega - V^{(0)} + \varepsilon_A, \tag{10}$$

$$V^{(0)} = \varepsilon_a. \tag{11}$$

Notice that the function T describes the process of scattering.

To obtain the Lorentz contour one has to insert the electron self-energy part in the internal electron line in Fig. 1. For simplicity we neglect the vacuum-polarization part. To the lowest order this leads to the graph depicted in Fig. 2 and the corresponding expression for the scattering amplitude evaluated within the resonance approximation takes the form

$$U_{Aa}^{(4)} = U_{Aa}^{(2)}\frac{V^{(1)}(\omega)}{\omega-\varepsilon_a+\varepsilon_A} = T^* D^{-1}\,[V^{(1)}(\omega)D^{-1}]T, \tag{12}$$

with

$$V^{(1)}(\omega) = e^2(\hat{\Sigma}_R(\omega+\varepsilon_A))_{aa}. \tag{13}$$

Here $\hat{\Sigma}_R(\omega)$ is the renormalized electron self-energy operator. The upper index at the function V indicates the order of perturbation theory with respect to powers of the fine-structure constant α for the graphs contributing to this function. Repeating these insertions in higher orders we can compose a geometric progression with the lth term:

$$Q_l = U_{Aa}^{(2)}\left[\frac{V^{(1)}(\omega)}{\omega-\varepsilon_a+\varepsilon_A}\right]^l = T^* D^{-1}[V^{(1)}(\omega)D^{-1}]^l\,T. \tag{14}$$

The resulting geometric progression is convergent for any ω except for values within the interval $\omega\in[\varepsilon_a-\varepsilon_A-|V^{(1)}|,\varepsilon_a-\varepsilon_A+|V^{(1)}|]$ close to the position of the resonance. Applying the formula for a convergent geometric progression one derives

$$U_{Aa} = \sum_{l=0}^{\infty} T^* D^{-1}\,[V^{(1)}(\omega)D^{-1}]^l\,T = \frac{T^*T}{D-V^{(1)}(\omega)} = \frac{T^*T}{\omega+\varepsilon_A-V^{(0)}-V^{(1)}(\omega)}. \tag{15}$$

Hence, the resonance is shifted into the complex plane and Eq. (15) is defined for all ω values on the real axis. Equation (15) presents the analytic continuation of the expansion $\Sigma_{l=0}^{\infty}Q_1$ to the entire complex plane.

Taking the square modulus of the amplitude (15), integrating over the directions of absorbed and emitted photons and summing over the polarizations we obtain the Lorentz profile for the absorption probability:

$$dW(\omega) = \frac{1}{2\pi}\times\frac{\Gamma_{aA}}{[\omega+\varepsilon_A-V^{(0)}-\mathrm{Re}\{V^{(1)}(\omega)\}]^2+[\mathrm{Im}\{V^{(1)}(\omega)\}]^2}\times d\omega. \tag{16}$$

Here $dW(\omega)$ is the probability for the absorption of a photon within the frequency interval $\omega,\omega+d\omega$ and Γ_{aA} is the partial width of the level a, associated with the transition $a\to A$.

Taking into account the correction depicted in Fig. 2 we improve the position of the resonance:

$$\omega^{\rm res} = -\varepsilon_A + V^{(0)} + \mathrm{Re}\{V^{(1)}(\varepsilon_a-\varepsilon_A)\} + O(\alpha^2). \tag{17}$$

Formula (16) defines the line profile of the process of scattering. Within the resonance approximation the line profile can be described by a Lorentz contour which is characterized by two parameters: the position of the resonance and the width. We define the energy shift for the state a as the shift of the resonance. The energy of the state a is

$$E = \omega^{\rm res}+\varepsilon_A = V^{(0)} + \mathrm{Re}\{V^{(1)}(\varepsilon_a-\varepsilon_A)\} + O(\alpha^2) \tag{18}$$

and the width of the level as the width of the corresponding Lorentz contour at the position of the resonance:

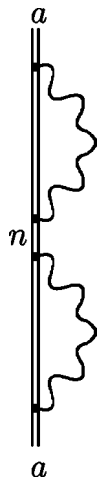

FIG. 3. The second-order electron self-energy correction (so-called SESE loop-after-loop) that gives rise to the correction in Eq. (25).

$$\Gamma = -2\ \mathrm{Im}\{V(\omega^{\mathrm{res}})\} = -2\ \mathrm{Im}\{V^{(1)}(\varepsilon_a - \varepsilon_A)\} + O(\alpha^2). \tag{19}$$

We note that the energy E of the level and its width Γ defined in the framework of the resonance approximation do not depend upon the function T (or Φ_A) and, therefore, they do not depend upon the type of scattering process. For example, we are free to consider not only the scattering of a photon but of some other particle as well which couples to electrons. Going beyond the resonance approximation the line profile can no longer be described by a Lorentz contour and, consequently, the energy level cannot be characterized only by two parameters E and Γ. In this case the evaluation of the energy levels should be replaced by the evaluation of the particular line profiles which, in general, depend upon the features of scattering process under consideration.

The real part of the matrix element $(\hat{\Sigma}_R(\varepsilon_a))_{aa}$ describes the lowest-order contribution to the Lamb shift, and the imaginary part, which is finite and not subject to renormalization, represents the total radiative (single-quantum) width of the level a:

$$\Delta E_a^{\mathrm{SE}} = (\hat{\Sigma}_R(\varepsilon_a))_{aa} = L_a^{\mathrm{SE}} - \frac{i}{2}\Gamma_a. \tag{20}$$

The other contribution to the lowest-order Lamb shift L_a^{VP} originates from the vacuum polarization. This correction does not contribute to the width Γ_a [6].

Studying the higher-order Lamb shift in one-electron atoms within the line profile approach, we have to account for the Feynman graph depicted in Fig. 3. For reasons of simplicity, we will not consider the other second-order graphs. In the case $n_1 = n_3 = a$ and $n_2 \neq a$ the graph in Fig. 4 can be viewed as a second-order self-energy insertion (loop-after-loop, irreducible part) in the graph in Fig. 1 within the resonance approximation. We derive the following expression for the scattering amplitude:

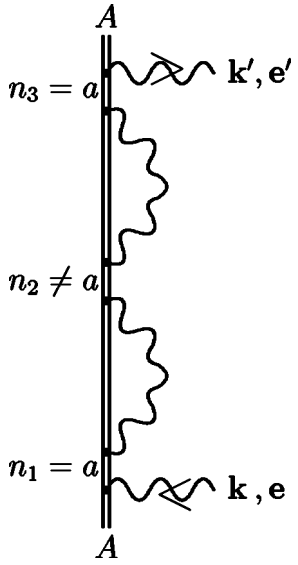

FIG. 4. Feynman graph representing the higher-order electron self-energy correction within the line profile approach (SESE, loop-after-loop, irreducible).

$$U_{Aa}^{(6)} = U_{Aa}^{(2)} \quad \frac{V^{(2)}(\omega)}{\omega - \varepsilon_a + \varepsilon_A} = T^{*} D^{-1}[V^{(2)}(\omega) D^{-1}]T, \tag{21}$$

where

$$V^{(2)}(\omega) = e^4 \sum_{n \neq a} \frac{(\hat{\Sigma}_R(\omega + \varepsilon_A))_{an} (\hat{\Sigma}_R(\omega + \varepsilon_A))_{na}}{\varepsilon_A - \varepsilon_n + \omega}. \tag{22}$$

Note that the singular term $n = a$ is not included here by definition. This term was taken into account in the geometric progression described above and represents exactly the second term of this progression. Repeating the evaluations leading to Eq. (16) with

$$Q_l = U_{Aa}^{(2)} \left(\frac{V^{(1)}(\omega) + V^{(2)}(\omega)}{\omega - \varepsilon_a + \varepsilon_A} \right)^l = T^{*} D^{-1} \{[V^{(1)}(\omega) + V^{(2)}(\omega)] D^{-1}\}^l T, \tag{23}$$

we obtain the improved resonance condition

$$V^{(0)} + \mathrm{Re}\{V^{(1)}(\omega^{\mathrm{res}}) + V^{(2)}(\omega^{\mathrm{res}})\} + O(\alpha^3) - \varepsilon_A - \omega^{\mathrm{res}} = 0. \tag{24}$$

Solving this equation for ω^{res} up to terms $O(\alpha^3)$ yields

$$\omega^{\mathrm{res}} = -\varepsilon_A + V^{(0)} + \mathrm{Re}\left\{ V^{(1)}(\varepsilon_a - \varepsilon_A) + V^{(2)}(\varepsilon_a - \varepsilon_A) + V^{(1)}(\varepsilon_a - \varepsilon_A) \left[\frac{\partial V^{(1)}(\omega)}{\partial \omega} \right]_{\omega = \varepsilon_a - \varepsilon_A} \right\} + O(\alpha^3). \tag{25}$$

The term $V^{(2)}(\varepsilon_a - \varepsilon_A)$ is the contribution of the irreducible part of the graph in Fig. 3. The derivative term corresponds to the reference state ($n = a$) correction. In particular, it coincides with the reference-state correction that arises from the

Feynman graph in Fig. 3 after application of the adiabatic *S*-matrix method [38]. The other second-order electron self-energy (SESE) corrections are irreducible [38].

B. Line profile approach for many-electron ions (nondegenerate energy level)

As in the one-electron case we will consider the process of photon scattering on an ion which is assumed to be in its lowest (ground) state. Investigating a nondegenerate energy level associated with a configuration containing at least one 1 *s* electron [such as $(1s2s)2\ ^1S_0$, $(1s2p_{1/2})2\ ^3P_0$, $(1s2s)2\ ^3S_1$, $(1s)^2\ 2s_{1/2}$, $(1s)^2\ 2p_{1/2}$, etc.] we can represent the wave function of the ground state via a proper combination of one-electron Dirac wave functions. A procedure based on this approach has been accomplished in [11,13]. However, for the investigation of quasidegenerate levels or a doubly excited level the interelectron interaction corrections have to be taken into account in the wave function of the ground state. Here we restrict ourselves to two-electron ions. The generalization to *N*-electron ions will be presented at the end of this section.

In the one-electron case we introduced the function Φ_A describing the process of scattering under consideration. To introduce such a function for the two-electron system we may consider first the simplest process of photon scattering on a two-electron ion, disregarding the interelectron interaction corrections to the initial (ground) state. This process is depicted in Fig. 5, where the ground state is represented by two noninteracting electrons, one of which absorbs (or emits) the photon. Accordingly, the ground-state wave function is given by

$$\Psi_A(x_1,x_2)=\frac{1}{\sqrt{2}}\ \det\{\psi_{1s}(x_1)\psi_{1s}(x_2)\}, \tag{26}$$

$$\overline{\Psi}_A(x_1,x_2)=\frac{1}{\sqrt{2}}\ \det\{\overline{\psi}_{1s}(x_1)\overline{\psi}_{1s}(x_2)\}, \tag{27}$$

where $\psi_{1s}(x_1)=\psi_{1s}(\mathbf{r}_1)\ e^{-i\varepsilon_{1s}t_1}$, $\psi_{1s}(x_2)$ are the Dirac one-electron functions with different projections of the total angular momentum. The bar over the one-electron functions indicates Dirac conjugation.

The *S*-matrix element corresponding to the graph in Fig. 5 can be written as

$$\begin{aligned}S_A^{(2)}=(-ie)^2\Bigg[&\int d^4x_{u_1}d^4x_{u_2}d^4x_{d_1}d^4x_{d_2}\delta^3(\mathbf{r}_{u_2}-\mathbf{r}_{d_2})\delta(t_{u_2})\delta(t_{d_2})d\omega_{n_1}\overline{\Psi}_A(x_{u_1},x_{u_2})\gamma^{\mu_{u_1}}A^{*(k',\lambda')}_{\mu_{u_1}}(x_{u_1})\\
&\times e^{-i\omega_{n_1}(t_{u_1}-t_{d_1})}\frac{i}{2\pi}\sum_{n_1}\frac{\psi_{n_1}(\mathbf{r}_{u_1})\overline{\psi}_{n_1}(\mathbf{r}_{d_1})}{\omega_{n_1}-\varepsilon_{n_1}(1-i0)}\gamma^{\mu_{d_1}}A^{(k,\lambda)}_{\mu_{d_1}}(x_{d_1})\Psi_A(x_{d_1},x_{d_2})+\int d^4x_{u_1}d^4x_{u_2}d^4x_{d_1}d^4x_{d_2}\delta^3(\mathbf{r}_{u_1}-\mathbf{r}_{d_1})\delta(t_{u_1})\delta(t_{d_1})d\omega_{n_2}\\
&\times\overline{\Psi}_A(x_{u_1},x_{u_2})\gamma^{\mu_{u_2}}A^{*(k',\lambda')}_{\mu_{u_2}}(x_{u_2})e^{-i\omega_{n_2}(t_{u_1}-t_{d_1})}\frac{i}{2\pi}\sum_{n_1}\frac{\psi_{n_2}(\mathbf{r}_{u_2})\overline{\psi}_{n_2}(\mathbf{r}_{d_2})}{\omega_{n_2}-\varepsilon_{n_2}(1-i0)}\gamma^{\mu_{d_2}}A^{(k,\lambda)}_{\mu_{d_2}}(x_{d_1},x_{d_2})\Bigg].\end{aligned} \tag{28}$$

In order to employ the functions Ψ_A and $\overline{\Psi}_A$ we introduced additional integrations $d^4x_{u_{1,2}}d^4x_{d_{1,2}}\delta^3(\mathbf{r}_{u_{1,2}}-\mathbf{r}_{d_{1,2}})\delta(t_{u_{1,2}})\delta(t_{d_{1,2}})$. The first and second terms in the square brackets represent graphs, where the photon is absorbed (emitted) by the first or by the second electron, respectively. Since the functions $\Psi_A(x_1,x_2)$ and $\overline{\Psi}_A(x_1,x_2)$ are antisymmetric it would be sufficient to consider one of these terms only.

As in the one-electron case we will look for the position of the resonance and employ the resonance approximation. It implies the neglect of the nonsingular terms (evaluated at the resonance) in comparison with singular ones. The terms in the sum over n_1 and n_2 in Eq. (28) may contain a singularity at the position of the resonance only if they correspond to the positive-energy part of the Dirac spectrum. Accordingly, in Eq. (28) we can restrict ourselves to terms with $\varepsilon_{n_1}>0, \varepsilon_{n_2}>0$.

Introducing the function $\Phi_A(x_1,x_2)$ as

$$\Phi_A(x_1,x_2)=\sqrt{2}\gamma^{\mu_1}A^{(k,\lambda)}_{\mu_1}(x_1)\Psi_A(x_1,x_2)\delta(t_1-t_2), \tag{29}$$

$$\overline{\Phi}_A(x_1,x_2)=\sqrt{2}\overline{\Psi}_A(x_1,x_2)\gamma^{\mu_1}A^{*(k',\lambda')}_{\mu_1}(x_1)\delta(t_1-t_2), \tag{30}$$

we can write

$$\begin{aligned}S_A^{(2)}=(-ie)^2\int d^4x_{u_1}d^4x_{u_2}d^4x_{d_1}d^4x_{d_2}d\omega_{n_1}d\omega_{n_2}\,\overline{\Phi}_A(x_{u_1},x_{u_2})\\
\times e^{-i\omega_{n1}(t_{u_1}-t_{d_1})}e^{-i\omega_{n_2}(t_{u_2}-t_{d_2})}\frac{i}{2\pi}\sum_{n_1}\frac{\psi_{n_1}(\mathbf{r}_{u_1})\overline{\psi}_{n_1}(\mathbf{r}_{d_1})}{\omega_{n_1}-\varepsilon_{n_1}(1-i0)}\\
\times\frac{i}{2\pi}\sum_{n_2}\frac{\psi_{n_2}(\mathbf{r}_{u_2})\overline{\psi}_{n_2}(\mathbf{r}_{d_2})}{\omega_{n_2}-\varepsilon_{n_2}(1-i0)}\Phi_A(x_{d_1},x_{d_2}).\end{aligned} \tag{31}$$

Here we can employ the identity

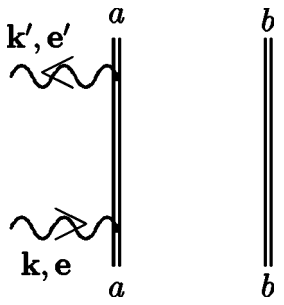

FIG. 5. Lowest-order amplitudes for photon scattering on a two-electron ion in its ground state A within the resonance approximation. The ground state A is represented in terms of noninteracting Dirac electrons.

$$\frac{1}{[\omega_{n_1}-\varepsilon_{n_1}(1-i0)]}\frac{1}{[\omega_{n_2}-\varepsilon_{n_2}(1-i0)]} = \frac{2\pi}{i}\frac{\delta(\omega_{n_1}-\varepsilon_{n_1})}{[\omega_{n_2}-\varepsilon_{n_2}(1-i0)]} + \frac{-1}{(-\omega_{n_1}+\varepsilon_{n_1}+i0\varepsilon_{n_1})[\omega_{n_2}-\varepsilon_{n_2}(1-i0)]}, \quad (32)$$

which follows from the Sokhotsky formulas

$$\frac{1}{x+i0} = -i\pi\delta(x)+\mathcal{P}\frac{1}{x}, \quad \frac{1}{x-i0} = i\pi\delta(x)+\mathcal{P}\frac{1}{x},$$

$$\frac{1}{x+i0}+\frac{1}{-x+i0} = \frac{2\pi}{i}\delta(x). \quad (33)$$

In view of the orthogonality of the Dirac functions and the asymmetry of the functions Ψ_A and $\overline{\Psi}_A$ the first term of Eq. (32) yields exactly Eq. (28). For $\varepsilon_{n_1}>0$ the second term of Eq. (32) does not contribute when inserted into Eq. (31). As was noticed above, for $\varepsilon_{n_1}<0$ the second term does not develop any singularity at the position of the resonance and can be disregarded.

Having performed the integration over the time variables $(t_{u_1}, t_{u_2}, t_{d_1}, t_{d_2})$ we arrive at

$$S_A^{(2)} = (-ie)^2(2\pi)^2\int d^3\mathbf{r}_{u_1}d^3\mathbf{r}_{u_2}d^3\mathbf{r}_{d_1}d^3\mathbf{r}_{d_2}\,d\omega_{n_1}d\omega_{n_2} \times\overline{\Phi}_A(\mathbf{r}_{u_1},\mathbf{r}_{u_2})\delta(\omega_{n_1}+\omega_{n_2}-E_A-\omega') \times\frac{i}{2\pi}\sum_{n_1}\frac{\psi_{n_1}(\mathbf{r}_{u_1})\overline{\psi}_{n_1}(\mathbf{r}_{d_1})}{\omega_{n_1}-\varepsilon_{n_1}(1-i0)}\frac{i}{2\pi}\sum_{n_2}\frac{\psi_{n_2}(\mathbf{r}_{u_2})\overline{\psi}_{n_2}(\mathbf{r}_{d_2})}{\omega_{n_2}-\varepsilon_{n_2}(1-i0)} \times\delta(E_A+\omega-\omega_{n_1}-\omega_{n_2})\Phi_A(\mathbf{r}_{d_1},\mathbf{r}_{d_2}), \quad (34)$$

where

$$\Phi_A(\mathbf{r}_1,\mathbf{r}_2) = \sqrt{2}\gamma^{\mu_1}A^{(k,\lambda)}_{\mu_1}(\mathbf{r}_1)\Psi_A(\mathbf{r}_1,\mathbf{r}_2), \quad (35)$$

$$\overline{\Phi}_A(\mathbf{r}_1,\mathbf{r}_2) = \sqrt{2}\overline{\Psi}_A(\mathbf{r}_1,\mathbf{r}_2)\gamma^{\mu_1}A^{*(k',\lambda')}_{\mu_1}(\mathbf{r}_1), \quad (36)$$

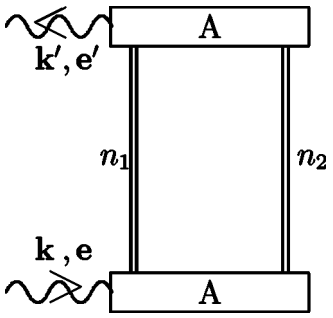

FIG. 6. The lowest-order amplitude for the photon scattering on a two-electron ion in the ground state A. In the ground state the interelectron interaction is taken into account.

$$E_A = \varepsilon_{1s}+\varepsilon_{1s}. \quad (37)$$

Formally the expression (34) is similar to the one in Eq. (4) which has been derived in the one-electron case. Taking into account interelectron interaction corrections to the ground state the function $\Phi_A(\mathbf{r}_1,\mathbf{r}_2)$ and the energy E_A will become more complicated in particular, the function $\Phi_A(\mathbf{r}_1,\mathbf{r}_2)$ will depend on ω_{n_1} and ω_{n_2}. Nevertheless, the form of the expression (34) would remain unchanged.

Below we will employ the resonance approximation defining the energy and width of the level such that they will not depend upon the features of the particular process of scattering. Since the function $\Phi_A(\mathbf{r}_1,\mathbf{r}_2)$ carries all information about the process of scattering, we can assume it to be arbitrary.

Accordingly, it is convenient to introduce a graphical designation: a rectangle with a letter A inside (see Fig. 6). Lower and upper rectangles represent the functions $\Phi_A(x_1,x_2)$ and $\overline{\Phi}_A(x_1,x_2)$, respectively, which are difined as

$$\Phi_A(x_1,x_2) = \Phi_A(\mathbf{r}_1,\mathbf{r}_2)e^{-it_1(E_A+\omega)}\delta(t_1-t_2), \quad (38)$$

$$\overline{\Phi}_A(x_1,x_2) = \overline{\Phi}_A(\mathbf{r}_1,\mathbf{r}_2)e^{it_1(E_A+\omega')}\delta(t_1-t_2). \quad (39)$$

Here $\Phi_A(\mathbf{r}_1,\mathbf{r}_2)$ denotes a complicated vertex function describing the scattering process under consideration, E_A is the

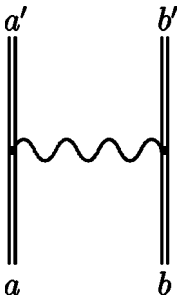

FIG. 7. Feynman graph, describing the first-order interelectron interaction. The double solid lines correspond to bound electrons in the field of the nucleus, and the wavy line corresponds to the exchange of virtual Coulomb and Breit (transverse) photons. For $a'=a$ and $b'=b$ the graph is called "direct," and for $a'=b, b'=a$ it is called an "exchange" graph, respectively.

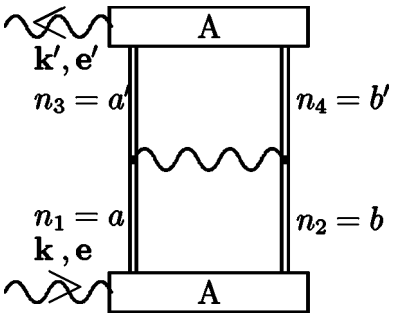

FIG. 8. First-order of interelectron interaction correction to the amplitude of the photon scattering on a two-electron ion within the resonance approximation.

energy of the ground state, and ω and ω' are the frequencies of the absorbed and emitted photons.

We will look for the position of a resonance near $\omega^{\mathrm{res}} = E^{(0)} - E_A + O(\alpha)$, where $E^{(0)} = \varepsilon_a + \varepsilon_b$ is the energy of two noninteracting electrons. Applying the identity (32) to Eq. (34) one can see that the δ-function term is singular close to the resonance, while the other term remains regular [here we assume the function $\Phi_A(\mathbf{r}_1, \mathbf{r}_2)$ to be arbitrary]. The resonance approximation implies the neglect of the nonsingular (at the resonance) terms in comparison with singular ones. Accordingly, within the framework of the resonance approximation the expression for the S matrix becomes

$$
\begin{aligned}
S_A^{(2)} = (-ie)^2 (2\pi)^2 \int & d^3\mathbf{r}_{u_1} d^3\mathbf{r}_{u_2} d^3\mathbf{r}_{d_1} d^3\mathbf{r}_{d_2} d\omega_{n_1} d\omega_{n_2} \\
& \times \overline{\Phi}_A(\mathbf{r}_{u_1}, \mathbf{r}_{u_2}) \delta(\omega_{n_1} + \omega_{n_2} - E_A - \omega') \delta(\omega_{n_1} - \varepsilon_{n_1}) \\
& \times \frac{i}{2\pi} \sum_{n_1, n_2} \frac{\psi_{n_1}(\mathbf{r}_{u_1}) \overline{\psi}_{n_1}(\mathbf{r}_{d_1}) \psi_{n_2}(\mathbf{r}_{u_2}) \overline{\psi}_{n_2}(\mathbf{r}_{d_2})}{\omega_{n_2} - \varepsilon_{n_2}(1 - i0)} \\
& \times \delta(E_A + \omega - \omega_{n_1} - \omega_{n_2}) \Phi_A(\mathbf{r}_{d_1}, \mathbf{r}_{d_2}). \qquad (40)
\end{aligned}
$$

Integrating over ω_{n_1} and ω_{n_2} in Eq. (40) and introducing the notation

$$
T_{n_1 n_2 A} = (-e) \int d^3\mathbf{r}_1 d^3\mathbf{r}_2 \, \overline{\psi}_{n_1}(\mathbf{r}_1) \overline{\psi}_{n_2}(\mathbf{r}_2) \Phi_A(\mathbf{r}_1, \mathbf{r}_2), \quad (41)
$$

we can express the corresponding amplitude for the scattering process in a form similar to Eq. (7):

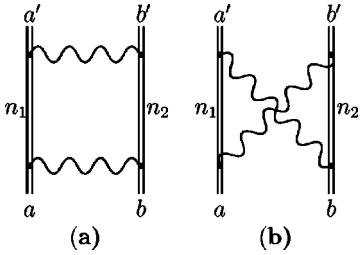

FIG. 9. Feynman graphs describing the second-order interelectron interaction. Graph (a) is called a "box" and graph (b) is called a "cross." Notations are the same as in Fig. 7. The summation over intermediate states is indicated by n_1, n_2.

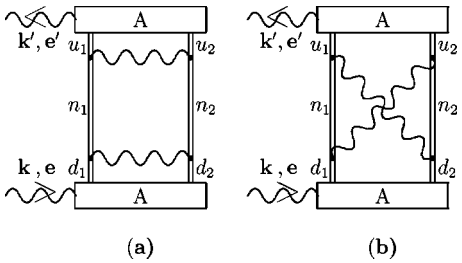

FIG. 10. Second-order of interelectron interaction correction to the amplitude of the photon scattering on a two-electron ion within the resonance approximation. Graph (a) represents the contribution of the "box" graph to the scattering amplitude, and graph (b) the contribution of the "cross" graph, respectively.

$$
U_A^{(2)} = \sum_{n_1 n_2} \frac{T^*_{A n_1 n_2} T_{n_1 n_2 A}}{\omega - \varepsilon_{n_1} - \varepsilon_{n_2} + E_A}. \qquad (42)
$$

Since we are searching for the position of the resonance near $\omega^{\mathrm{res}} = E^{(0)} - E_A + O(\alpha)$, we have to retain only terms in the denominator of Eq. (42) for which $\varepsilon_{n_1} + \varepsilon_{n_2} = E^{(0)}$. We assume the energy level close to $E^{(0)} = \varepsilon_a + \varepsilon_b$ to be nondegenerate and hence, within the resonance approximation the amplitude takes the form

$$
U_A^{(2)} = \sum_{n_1 n_2} \frac{T^*_{A n_1 n_2} T_{n_1 n_2 A}}{\omega - E^{(0)} + E_A} = T^+ D^{-1} T. \qquad (43)
$$

Here the summations run only over quantum numbers n_1 and n_2, satisfying the condition $\varepsilon_{n_1} + \varepsilon_{n_2} = E^{(0)}$. The matrices T and D^{-1} are given by

$$
(T)_{n_1 n_2} = T_{n_1 n_2 A}, \qquad (44)
$$

$$
(D)_{n_1 n_2} = \omega - V^{(0)} + E_A, \qquad (45)
$$

together with

$$
V^{(0)} = E^{(0)}. \qquad (46)
$$

As in the one-electron case T defines the type of scattering process under consideration.

The interelectron interaction correction in first order is represented by the graph in Fig. 7. In order to evaluate this contribution which also shifts the position the resonance, one has to consider the graph in Fig. 8. In this paper we employ the Coulomb gauge together with the covariant metric. The photon propagator can be written as

$$D^{\mathrm{c,t}}_{\mu_1\mu_2}(x_1,x_2)=\frac{i}{2\pi}\int_{-\infty}^{\infty}d\,\Omega\; I^{\mathrm{c,t}}_{\mu_1\mu_2}(|\,\Omega\,|,r_{12})e^{-i\Omega(t_1-t_2)}, \tag{47}$$

where $r_{12}=|\mathbf{r}_1-\mathbf{r}_2|$ and

$$I^{\mathrm{c}}_{\mu_1\mu_2}(\Omega,r_{12})=\frac{\delta_{\mu_1 0}\delta_{\mu_2 0}}{r_{12}}, \tag{48}$$

$$I^{\mathrm{t}}_{\mu_1\mu_2}(\Omega,r_{12})=-\left(\frac{\delta_{\mu_1\mu_2}}{r_{12}}e^{i\Omega r_{12}}+\frac{\partial}{\partial x_1^{\mu_1}}\frac{\partial}{\partial x_2^{\mu_2}}\frac{1}{r_{12}}\frac{1-e^{i\Omega r_{12}}}{\Omega^2}\right)\times(1-\delta_{\mu_1 0})(1-\delta_{\mu_2 0}). \tag{49}$$

The propagator $D^{\mathrm{c}}_{\mu_1\mu_2}(x_1,x_2)$ corresponds to Coulomb photons, while $D^{\mathrm{t}}_{\mu_1\mu_2}(x_1,x_2)$ describes transverse (Breit) photons. The neglect of retardation implies the substitution $I^{\mathrm{t}}_{\mu_1\mu_2}(\Omega,r_{12})=I^{\mathrm{t}}_{\mu_1\mu_2}(0,r_{12})$. We employ also the notation

$$I^{\mathrm{c,t}}(\Omega)_{a'b'ab}=\sum_{\mu_1\mu_2}\int d^3\mathbf{r}_1 d^3\mathbf{r}_2\, I^{\mathrm{c,t}}_{\mu_1\mu_2}(\Omega,r_{12})\times\langle\overline{\psi}_{a'}(\mathbf{r}_1)\gamma^{\mu_1}\psi_a(\mathbf{r}_1)\rangle\langle\overline{\psi}_{b'}(\mathbf{r}_2)\gamma^{\mu_2}\psi_b(\mathbf{r}_2)\rangle. \tag{50}$$

The Lorentz indices μ_i should indicate that the Dirac matrices γ^{μ_i} act on Dirac wave functions depending on variables $\mathbf{r}_i$. The corresponding S-matrix element reads

$$\begin{aligned}S_A^{(4)}=(-ie)^4\int d^4x_1 d^4x_2 d\,\Omega\, d^4x_{u_1}d^4x_{u_2}d^4x_{d_1}d^4x_{d_2}d\omega_{u_1}d\omega_{u_2}d\omega_{d_1}d\omega_{d_2}\overline{\Phi}_A(\mathbf{r}_{u_1},\mathbf{r}_{u_2})e^{it_{u_1}(E_A+\omega')}\delta(t_{u_1}-t_{u_2})\frac{i}{2\pi}\\ \times\sum_{u_1}\frac{\psi_{u_1}(\mathbf{r}_{u_1})\overline{\psi}_{u_1}(\mathbf{r}_1)}{\omega_{u_1}-\varepsilon_{u_1}(1-i0)}\frac{i}{2\pi}\sum_{u_2}\frac{\psi_{u_2}(\mathbf{r}_{u_2})\overline{\psi}_{u_2}(\mathbf{r}_2)}{\omega_{u_2}-\varepsilon_{u_2}(1-i0)}e^{-i\omega_{u_1}(t_{u_1}-t_1)}e^{-i\omega_{u_2}(t_{u_2}-t_2)}e^{-i\omega_{d_1}(t_1-t_{d_1})}e^{-i\omega_{d_2}(t_2-t_{d_2})}\gamma^{\mu_1}\gamma^{\mu_2}\frac{i}{2\pi}\\ \times\sum_{d_1}\frac{\psi_{d_1}(\mathbf{r}_1)\overline{\psi}_{d_1}(\mathbf{r}_{d_1})}{\omega_{d_1}-\varepsilon_{d_1}(1-i0)}\frac{i}{2\pi}\sum_{d_2}\frac{\psi_{d_2}(\mathbf{r}_2)\overline{\psi}_{d_2}(\mathbf{r}_{d_2})}{\omega_{d_2}-\varepsilon_{d_2}(1-i0)}\frac{i}{2\pi}I_{\mu_1\mu_2}(|\,\Omega\,|,r_{12})e^{-i\Omega(t_1-t_2)}e^{-it_{d_1}(E_A+\omega)}\delta(t_{d_1}-t_{d_2})\Phi_A(\mathbf{r}_{d_1},\mathbf{r}_{d_2}),\end{aligned} \tag{51}$$

while the summations over u_1,u_2 and d_1,d_2 run over the entire Dirac spectrum. Employing the identity (32) and retaining only terms which are singular near the resonance—i.e., keeping δ-function terms Eq. (32) only—we obtain

$$S_A^{(4)}=-2\pi i\delta(\omega-\omega')U^{(4)}=-2\pi i\delta(\omega-\omega')\sum_{u_1u_2d_1d_2}T^{+}_{Au_1u_2}\frac{1}{E_A+\omega-\varepsilon_{u_1}-\varepsilon_{u_2}}e^2I(|-\varepsilon_{d_1}+\varepsilon_{u_1}|)_{u_1u_2d_1d_2}\frac{1}{E_A+\omega-\varepsilon_{d_1}-\varepsilon_{d_2}}T_{d_1d_2A}. \tag{52}$$

Within the resonance approximation we are left with terms satisfying the condition $\varepsilon_{u_1}+\varepsilon_{u_2}=\varepsilon_{d_1}+\varepsilon_{d_2}=E^{(0)}$.

The second-order interelectron interaction correction is represented by the graphs in Fig. 9. In order to apply the line profile approach to the contribution of the "box" graph of Fig. 9 we have to consider the graph depicted in Fig. 10(a). The corresponding S-matrix element reads

$$\begin{aligned}S_A^{(6)}=(-ie)^2\int d^4x_1 d^4x_2 d^4x_3 d^4x_4 d\,\Omega\, d\,\Xi\, d^4x_{u_1}d^4x_{u_2}d^4x_{d_1}d^4x_{d_2}d\omega_{u_1}d\omega_{u_2}d\omega_{d_1}d\omega_{d_2}\overline{\Phi}_A(\mathbf{r}_{u_1},\mathbf{r}_{u_2})e^{it_{u_1}(E_A+\omega')}\delta(t_{u_1}-t_{u_2})\frac{i}{2\pi}\\ \times\sum_{u_1}\frac{\psi_{u_1}(\mathbf{r}_{u_1})\overline{\psi}_{u_1}(\mathbf{r}_3)}{\omega_{u_1}-\varepsilon_{u_1}(1-i0)}\frac{i}{2\pi}\sum_{u_2}\frac{\psi_{u_2}(\mathbf{r}_{u_2})\overline{\psi}_{u_2}(\mathbf{r}_4)}{\omega_{u_2}-\varepsilon_{u_2}(1-i0)}e^{-i\omega_{u_1}(t_{u_1}-t_3)}e^{-i\omega_{u_2}(t_{u_2}-t_4)}e^{-i\omega_{n_1}(t_3-t_1)}e^{-i\omega_{n_2}(t_4-t_2)}\gamma^{\mu_3}\gamma^{\mu_4}\frac{i}{2\pi}\\ \times\sum_{n_1}\frac{\psi_{n_1}(\mathbf{r}_3)\overline{\psi}_{n_1}(\mathbf{r}_1)}{\omega_{n_1}-\varepsilon_{n_1}(1-i0)}\frac{i}{2\pi}\sum_{n_2}\frac{\psi_{n_2}(\mathbf{r}_4)\overline{\psi}_{n_2}(\mathbf{r}_2)}{\omega_{n_2}-\varepsilon_{n_2}(1-i0)}e^{-i\omega_{d_1}(t_1-t_{d_1})}e^{-i\omega_{d_2}(t_2-t_{d_2})}\gamma^{\mu_1}\gamma^{\mu_2}\frac{i}{2\pi}\sum_{d_1}\frac{\psi_{d_1}(\mathbf{r}_1)\overline{\psi}_{d_1}(\mathbf{r}_{d_1})}{\omega_{d_1}-\varepsilon_{d_1}(1-i0)}\frac{i}{2\pi}\\ \times\sum_{d_2}\frac{\psi_{d_2}(\mathbf{r}_2)\overline{\psi}_{d_2}(\mathbf{r}_{d_2})}{\omega_{d_2}-\varepsilon_{d_2}(1-i0)}\frac{i}{2\pi}I_{\mu_1\mu_2}(|\,\Xi\,|,r_{12})e^{-i\Xi(t_1-t_2)}\frac{i}{2\pi}I_{\mu_3\mu_4}(|\,\Omega\,|,r_{34})e^{-i\Omega(t_3-t_4)}e^{-it_{d_1}(E_A+\omega)}\delta(t_{d_1}-t_{d_2})\Phi_A(\mathbf{r}_{d_1},\mathbf{r}_{d_2}).\end{aligned} \tag{53}$$

Employing the identity (32) and retaining only the terms in the summation over u_1,u_2 and d_1,d_2 which become singular close to the resonance, we obtain the following expression for the S-matrix element corresponding to the graph in Fig. 9(a):

$$S_A^{(6)} = -2\pi i\delta(\omega-\omega')U^{(6)} = -2\pi i\delta(\omega-\omega')\sum_{u_1u_2d_1d_2} T^{+}_{Au_1u_2}\frac{1}{E_A+\omega-\varepsilon_{u_1}-\varepsilon_{u_2}}e^4\frac{i}{2\pi}$$
$$\times\sum_{n_1n_2}\int d\,\Omega\,\frac{I(|\,\Omega\,|)_{u_1u_2n_1n_2}I(|-\,\Omega-\varepsilon_{d_1}+\varepsilon_{u_1}|)_{n_1n_2d_1d_2}}{[-\,\Omega\,+\varepsilon_{u_1}+\varepsilon_{n_1}(1-i0)][E_A+\omega+\,\Omega-\varepsilon_{u_1}-\varepsilon_{n_2}(1-i0)]}\,\frac{1}{E_A+\omega-\varepsilon_{d_1}-\varepsilon_{d_2}}T_{d_1d_2A}. \tag{54}$$

Again within the resonance approximation only terms satisfying the condition $\varepsilon_{u_1}+\varepsilon_{u_2}=\varepsilon_{d_1}+\varepsilon_{d_2}=E^{(0)}$ will be kept in the summations over u_1,u_2 and d_1,d_2.

Let us consider separately the reference states terms—i.e., for which $\varepsilon_{n_1}+\varepsilon_{n_2}=E^{(0)}$ holds. Inserting a similar identity for the energy denominators

$$\frac{1}{[-\,\Omega\,+\varepsilon_{u_1}-\varepsilon_{n_1}(1-i0)][E_A+\omega+\,\Omega-\varepsilon_{u_1}-\varepsilon_{n_2}(1-i0)]}$$
$$=\frac{2\pi}{i}\frac{\delta(\Omega-\varepsilon_{u_1}+\varepsilon_{n_1})}{(E_A+\omega-\varepsilon_{n_1}-\varepsilon_{n_2})}+\frac{-1}{(\Omega-\varepsilon_{u_1}+\varepsilon_{n_1}+\varepsilon_{n_1}i0)[E_A+\omega+\,\Omega-\varepsilon_{u_1}-\varepsilon_{n_2}(1-i0)]}, \tag{55}$$

into Eq. (54), one can verify that the term with the δ function coincides with the second element of the geometric progression for the graph in Fig. 7. Hence, while generating the geometric progression this term will refer to the second element of the progression.

In order to evaluate rigorously the position of the resonance up to second order in α we have to consider all corrections of first and second order simultaneously. Up to first order of perturbation theory we have to account for SE and VP corrections as well as for the exchange of one Coulomb or one Breit photon. In second order we have to account for all one- and two-electron Feynman graphs of second order including radiative corrections, screening of the self-energy and vacuum polarization, and two-photon exchange graphs. However, the evaluation of the radiative corrections is not the goal of the present work. Below we will present the derivation of a formula for the one-photon exchange contribution in Fig. 7, the two-photon exchange "box" graph in Fig. 9(a) and the three-photon exchange "box" graph Fig. 11.

The scattering amplitude can be written as

$$U_{Aa}^{(4)} = T^{+}D^{-1}[(V^{(1)}+V^{(2)}+V^{(3)})D^{-1}]T, \tag{56}$$

where $V^{(1)}$ corresponds to the one-photon exchange graph Fig. 7 [see Eq. (52)]:

$$V^{(1)} = e^2\sum_{\mathrm{g=c,t}} I^{\mathrm{g}}(|-\varepsilon_a+\varepsilon_{a'}|)_{a'b'ab}. \tag{57}$$

In contrast to the one-electron radiative corrections [see formula (13)], this one-photon exchange correction does not depend on ω. Taking into account the "box" graph in Fig. 9(a) we obtain [see formulas (54) and (55)]

$$V^{(2)}(\omega) = e^4\frac{i}{2\pi}\sum_{\mathrm{gg'=c,t}}\sum_{\varepsilon_{n_1}+\varepsilon_{n_2}\neq\varepsilon_a+\varepsilon_b}\int_{-\infty}^{\infty} d\,\Omega\, I^{\mathrm{g}}(|\,\Omega\,|)_{a'b'n_1n_2}I^{\mathrm{g'}}(|-\,\Omega-\varepsilon_a+\varepsilon_{a'}|)_{n_1n_2ab}$$
$$\times\frac{1}{[-\,\Omega\,+\varepsilon_{a'}-\varepsilon_{n_1}(1-i0)][E_A+\omega+\,\Omega-\varepsilon_{a'}-\varepsilon_{n_2}(1-i0)]}+e^4\frac{i}{2\pi}\sum_{\mathrm{gg'=c,t}}\sum_{\varepsilon_{n_1}+\varepsilon_{n_2}=\varepsilon_a+\varepsilon_b}\int_{-\infty}^{\infty} d\,\Omega$$
$$\times I^{\mathrm{g}}(|\,\Omega\,|)_{a'b'n_1n_2}I^{\mathrm{g'}}(|-\,\Omega-\varepsilon_a+\varepsilon_{a'}|)_{n_1n_2ab}\frac{-1}{(\Omega-\varepsilon_{a'}+\varepsilon_{n_1}+\varepsilon_{n_1}i0)[E_A+\omega+\,\Omega-\varepsilon_{a'}-\varepsilon_{n_2}(1-i0)]}. \tag{58}$$

Again the summations over g and g′ run over scalar (Coulomb) and transverse (Breit) photons, respectively. The second term in Eq. (58) represents the remainder after subtracting off the reference-state singularity. This subtraction was done at the stage of generating the geometric progression with the one-photon exchange insertion. In particular, the identity (55) was employed for deriving the expression for the reference-state contribution (the reducible part) of the

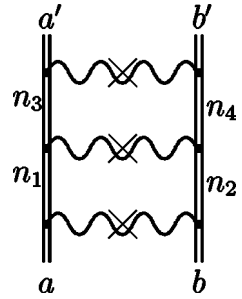

FIG. 11. The third-order "box" Feynman graph. The notations are the same as in Fig. 7. Here the wavy lines with the cross represent the sum of the Coulomb and unretarded Breit interactions.

"box" graph, where the δ-function term coincides with the second element of geometric progression for the one-photon exchange graph.

In the case of one-electron ions the reference-state term [see Eq. (22)] appeared only via the derivative term in Eq. (25). Considering photon exchange in two-electron ions the situation is different. In this case a reference-state contribution appears directly in $V^{(2)}(\omega)$ [see Eq. (58)] while a derivative term does not arise since $V^{(1)}$ does not depend on ω. Nevertheless, if the sets $\{a,b\}$ and $\{a',b'\}$ are equivalent, the term corresponding to the reference states can be expressed as a derivative. At the point of the resonance we can set $\omega = -E_A + E^{(0)}$ in Eq. (58). Accordingly, both factors in the denominator will be identical. Utilizing the formula

$$\frac{-1}{(x+i0)^2} = \frac{d}{dx}\frac{1}{(x+i0)} \tag{59}$$

and integrating by parts we can shift the derivative to $I(\Omega)$.

Let us now turn to the three-photon exchange correction neglecting retardation effects, crossed-photon graphs, and the contribution of the negative-energy part of the Dirac spectrum. Within this approximation the photon propagator does not depend on the frequency Ω, which yields

$$V^{(3)}(\omega) = \sum_{\mathrm{gg'g''=c,t}} {\sum_{n_1 n_2 n_3 n_4}}' I^{\mathrm{g}}_{a'b'n_3n_4} I^{\mathrm{g'}}_{n_3n_4n_1n_2} I^{\mathrm{g''}}_{n_1n_2ab} \times \frac{1}{(\varepsilon_{n_3}+\varepsilon_{n_4}-E_A-\omega)(\varepsilon_{n_1}+\varepsilon_{n_2}-E_A-\omega)}, \tag{60}$$

where the prime at the summation symbol indicates that the reference states ($\varepsilon_{n_1}+\varepsilon_{n_2}=\varepsilon_a+\varepsilon_b, \varepsilon_{n_3}+\varepsilon_{n_4}=\varepsilon_a+\varepsilon_b$) are omitted.

Taking together the contributions of $V^{(1)}, V^{(2)}$, and $V^{(3)}$, we can generate a geometric progression, where the lth term reads

$$Q_l = T^{+}D^{-1}[(V^{(1)}+V^{(2)}+V^{(3)})D^{-1}]^l T. \tag{61}$$

Performing similar steps as in the one-electron case we sum up this progression and derive a condition for the position of the resonance:

$$V^{(0)} + \mathrm{Re}\{V^{(1)}(\omega^{\mathrm{res}}) + V^{(2)}(\omega^{\mathrm{res}}) + V^{(3)}(\omega^{\mathrm{res}})\} - \varepsilon_A - \omega^{\mathrm{res}} = 0. \tag{62}$$

The energy and width of the level will be equal to [see Eqs. (18) and (19)]

$$E = V^{(0)} + \mathrm{Re}\{V^{(1)}(\omega^{\mathrm{res}}) + V^{(2)}(\omega^{\mathrm{res}}) + V^{(3)}(\omega^{\mathrm{res}})\} + O(\alpha^4), \tag{63}$$

$$\Gamma = -2\,\mathrm{Im}\{V^{(1)}(\omega^{\mathrm{res}}) + V^{(2)}(\omega^{\mathrm{res}}) + V^{(3)}(\omega^{\mathrm{res}})\} + O(\alpha^4). \tag{64}$$

It is important to emphasize that Eq. (64) has the meaning of a correction to the width of the level only if the full set of Feynman graphs of a given order is under consideration. Indeed, the contribution of the graph in Fig. 7 cancels completely with a part of the contribution of the self-energy correction, while the vacuum polarization gives zero contribution to the width. Such a cancellation is an immediate consequence of the Pauli principle according to which transitions of electrons into occupied states are prohibited [39].

We note that the two-electron graphs to the first order in $V^{(1)}$ do not depend on ω. Hence, the solution of Eq. (62) together with $V^{(1)}$, $V^{(2)}$, and $V^{(3)}$ given by Eqs. (57), (58) and (60) yields

$$\omega^{\mathrm{res}} = -E_A + V^{(0)} + \mathrm{Re}\left\{ V^{(1)}(E^{(0)}-E_A) + V^{(2)}(E^{(0)}-E_A) + V^{(3)}(E^{(0)}-E_A) + V^{(1)}(E^{(0)}-E_A) \times \left[\frac{\partial V^{(2)}(\omega)}{\partial \omega}\right]_{\omega=E^{(0)}-E_A}\right\} + O(\alpha^4). \tag{65}$$

The term $V^{(1)}(\varepsilon_a-\varepsilon_A)$ represents the contribution of one-photon exchange graph in Fig. 7, while the term $V^{(2)}(\varepsilon_a-\varepsilon_A)$ accounts for the contribution of the two-photon exchange graphs in Fig. 9. In particular, this term includes the contribution of the reference states occurring in these graphs. The third-order term $V^{(3)}(\varepsilon_a-\varepsilon_A)$ contributes to the three-photon exchange graphs in Fig. 11. It does not contain the contribution of the reference states because we disregard retardation effects, considering it within the framework of RMBPT. The derivative term in Eq. (65) as well as that term in Eq. (25) does not correspond to a certain Feynman graph. Similar to Eq. (25) it can be related to the contribution of the reducible part (reference states) of the graph in Fig. 11.

Let us mention that if we would take into account in addition the radiative corrections and as well as screening effects, we would obtain a corresponding correction $V^{(1)}(\omega)$ containing the contribution of the electron self-energy (13), the one-photon exchange (57), and vacuum polarization. For $V^{(2)}(\omega)$ we would similarly obtain the sum of Eqs. (22) and (58) and in addition all the missing radiative effects of second order together with the screened self-energy and vacuum-polarization corrections. Accordingly, instead of Eq. (65) we would have been left with

$$\omega^{\rm res} = -E_A + V^{(0)} + {\rm Re}\Bigg\{ V^{(1)}(E^{(0)}-E_A) + V^{(2)}(E^{(0)}-E_A) + V^{(1)}(E^{(0)}-E_A)\left[\frac{\partial V^{(1)}(\omega)}{\partial\omega}\right]_{\omega=E^{(0)}-E_A} + V^{(3)}(E^{(0)}-E_A)$$
$$+\frac{1}{2}V^{(1)}(E^{(0)}-E_A)^2\left[\frac{\partial^2 V^{(1)}(\omega)}{\partial\omega^2}\right]_{\omega=E^{(0)}-E_A} + V^{(1)}(E^{(0)}-E_A)\left[\frac{\partial V^{(1)}(\omega)}{\partial\omega}\right]^2_{\omega=E^{(0)}-E_A} + V^{(1)}(E^{(0)}-E_A)\left[\frac{\partial V^{(2)}(\omega)}{\partial\omega}\right]_{\omega=E^{(0)}-E_A}$$
$$+V^{(2)}(E^{(0)}-E_A)\left[\frac{\partial V^{(1)}(\omega)}{\partial\omega}\right]_{\omega=E^{(0)}-E_A}\Bigg\} + O(\alpha^4). \tag{66}$$

Formulating the line profile approach for N-electron ions, it might be convenient to introduce the function

$$\Phi_A(x_1,\ldots,x_N) = \Phi_A(\mathbf{r}_1,\ldots,\mathbf{r}_N)e^{-it_1(E_A+\omega)}\prod_{j=2}^{N}\delta(t_1-t_j), \tag{67}$$

which should be depicted graphically by a rectangle with a letter A inside and with N outgoing electron lines. Here $\Phi_A(\mathbf{r}_1,\ldots,\mathbf{r}_N)$ describes the N-electron ions in the lowest (ground) state A together with the absorbed photon. Accordingly, formula (32) generalizes to

$$\prod_{j=1}^{N}\frac{1}{[\omega_{n_j}-\varepsilon_{n_j}(1-i0)]} = \left[\prod_{j=1}^{N-1}\left(\frac{2\pi}{i}\delta(\omega_{n_j}-\varepsilon_{n_j})+\frac{-1}{(-\omega_{n_j}+\varepsilon_{n_j}+i0\varepsilon_{n_j})}\right)\right] \times\frac{1}{[\omega_{n_N}-\varepsilon_{n_N}(1-i0)]}. \tag{68}$$

This identity can be written as

$$\prod_{j=1}^{N}\frac{1}{[\omega_{n_j}-\varepsilon_{n_j}(1-i0)]} = \frac{\prod_{j=1}^{N-1}\frac{2\pi}{i}\delta(\omega_{n_j}-\varepsilon_{n_j})}{[\omega_{n_N}-\varepsilon_{n_N}(1-i0)]} + f(\omega,\varepsilon). \tag{69}$$

Then the terms in Eqs. (34), (51), and (53) which correspond to the function $f(\omega,\varepsilon)$ will not contain the singularities and will be omitted within the framework of the resonance approximation. Equations (65) and (66) will remain unchanged however, now V will contain additional contributions of three- and up to N-electron graphs. In particular, for three-electron ions the functions $V^{(2)}(\omega)$ and $V^{(3)}(\omega)$ will also account for contributions of three-electron graphs (see [11]).

C. Line profile approach for many-electron ions (quasidegenerate energy levels)

We now turn to the application of the line profile approach to quasidegenerate levels. Without loss of generality, we can restrict ourselves to two mixing configurations. We will search for the positions of the resonances corresponding to these configurations and will construct basic wave functions Ψ_1 and Ψ_2 within the $j-j$ coupling scheme. The energies corresponding to these wave functions are denoted by $E_1^{(0)}$ and $E_2^{(0)}$, and they are supposed to be close to the exact energies of the electron configurations under consideration. Employing the line profile approach we will consider a scattering of a photon on a two-electron ion in its ground state A. The positions of resonances may be found near the values $\omega_1^{\rm res}=E_1^{(0)}-E_A+O(\alpha)$ and $\omega_2^{\rm res}=E_2^{(0)}-E_A+O(\alpha)$, respectively. Within the resonance approximation we will have to retain two terms in the sum (42) corresponding to the basic functions Ψ_1 and Ψ_2. The scattering amplitude may be written as

$$U_{Aa} = T^{+}D^{-1}[\Delta V D^{-1}]T, \tag{70}$$

where D is a matrix 2×2, defined on the functions Ψ_1,Ψ_2:

$$D = \omega + E_A - V^{(0)}, \tag{71}$$

$$V^{(0)} = \hat{h}_1 + \hat{h}_2, \tag{72}$$

$$\Delta V = V - V^{(0)} = V^{(1)} + V^{(2)} + V^{(3)} + \cdots. \tag{73}$$

Here $\hat{h}_1$ and $\hat{h}_2$ are the one-electron Dirac Hamiltonians acting on the one-electron Dirac wave functions depending on $\mathbf{r}_1$ or $\mathbf{r}_2$, respectively. Since the functions Ψ_1 and Ψ_2 are orthogonal, the matrix D is diagonal. Accordingly, we now have to compose a geometric matrix progression with the lth term

$$Q_l = T^{+}D^{-1}[\Delta V D^{-1}]^l T \tag{74}$$

and sum it up employing the formula for a convergent geometric progression. The expression for the amplitude reads

$$U_A = T^{+}[D-\Delta V]^{-1}T \equiv T^{+}\frac{1}{D-\Delta V}T = T^{+}\frac{1}{\omega+E_A-V}T. \tag{75}$$

Introducing the function $\mathbf{\Phi}=(\Phi_1,\Phi_2)$ by means of the relation $\mathbf{\Phi}=B\Psi$, where the matrix B is assumed to diagonalize the matrix $V=V^{(0)}+\Delta V$—i.e. $V^{\rm diag}=B^{+}VB$. The expression for the amplitude can now be written in the form

$$U_A = T^+_{A\Phi_1} \frac{1}{\omega + E_A - [B^+VB]_{\Phi_1\Phi_1}} T_{\Phi_1 A} + T^+_{A\Phi_2} \frac{1}{\omega + E_A - [B^+VB]_{\Phi_2\Phi_2}} T_{\Phi_2 A} = T^+_{A\Phi_1} \frac{1}{\omega + E_A - V^{\rm diag}_{\Phi_1\Phi_1}(\omega)} T_{\Phi_1 A} + T^+_{A\Phi_2} \frac{1}{\omega + E_A - V^{\rm diag}_{\Phi_2\Phi_2}(\omega)} T_{\Phi_2 A}. \quad (76)$$

Taking a square modulus of the amplitude (76) and integrating over the directions of the absorbed and emitted photons yields a line profile for the probability of photon absorption. The positions of the resonances are determined by the equations

$$\omega_1^{\rm res} + E_A - {\rm Re}\{V^{\rm diag}_{\Phi_1\Phi_1}(\omega_1^{\rm res})\} = 0, \quad (77)$$

$$\omega_2^{\rm res} + E_A - {\rm Re}\{V^{\rm diag}_{\Phi_2\Phi_2}(\omega_2^{\rm res})\} = 0. \quad (78)$$

Hence, the energies of the configurations are

$$E_{\Phi_1} = {\rm Re}\{V^{\rm diag}_{\Phi_1\Phi_1}(\omega_1^{\rm res})\}, \quad (79)$$

$$E_{\Phi_2} = {\rm Re}\{V^{\rm diag}_{\Phi_2\Phi_2}(\omega_2^{\rm res})\}. \quad (80)$$

Assuming that the energies of the configurations are close to each other, we can expand Eqs. (77) and (78) into a Taylor series around the values $\omega_1^{\rm res} = -E_A + E_1^{(0)}$ and $\omega_2^{\rm res} = -E_A + E_2^{(0)}$, respectively. As in the case of nondegenerate levels this can be achieved up to any desired accuracy.

Note that employing the resonance approximation in case of nondegenerate level we have to retain in a corresponding sum (42) certain many-electron functions composed within the $j-j$ coupling scheme. Indeed, after diagonalization of the matrix V all other combinations of one-electron functions will yield zero in view of the antisymmetry of the wave function of the ground state and the symmetry of the matrix V. Hence, having constructed a many-electron function in the $j-j$ coupling scheme, Eq. (56) becomes a scalar one.

The line profile approach outlined above can be easily employed for an arbitrary number of degenerate levels. The generalization of the method to N-electron ions was described at the end of the previous section.

III. EVALUATION OF THE ENERGY LEVELS OF QUASIDEGENERATE TWO-ELECTRON CONFIGURATIONS

We will evaluate the interelectron interaction correction for the two-electron configurations $(1s2p)2^1P_1$ and $(1s2p)2^3P_1$. Employing the relativistic $j-j$ coupling scheme these energy levels become quasidegenerate in the region $Z \leqslant 40$. To treat such states within the framework of QED we will apply the line profile approach. Within the $j-j$ coupling scheme the wave function of a two-electron configuration can be represented as

$$\Psi_{JMj_1j_2l_1l_2}(\mathbf{r}_1,\mathbf{r}_2) = N \sum_{m_1,m_2} C^{j_1j_2}_{JM}(m_1m_2) \times [\psi_{j_1l_1m_1}(\mathbf{r}_1)\psi_{j_2l_2m_2}(\mathbf{r}_2) - \psi_{j_1l_1m_1}(\mathbf{r}_2)\psi_{j_2l_2m_2}(\mathbf{r}_1)], \quad (81)$$

where the normalization constant is $N=1/2$ for equivalent electrons and $N=1/\sqrt{2}$ for nonequivalent electrons, respectively. $C^{j_1j_2}_{JM}(m_1m_2)$ is a Clebsch-Gordan coefficient. The one-electron Dirac functions $\psi_{jlm}(\mathbf{r})$ are characterized by the standard set of one-electron quantum numbers—total angular momentum j, its projection m, and the orbital angular momentum l—that fix the parity of the state. For the two-electron wave function the relevant quantum numbers are the total angular momentum J and its projection M.

Following the procedure described in Sec. II C we will construct the matrix V, Eq. (73), on the functions (81),

$$\Psi_{J=1,M=0,j_1=1/2,j_2=1/2,l_1=0,l_2=1} \equiv (1s2p_{1/2}), \quad (82)$$

$$\Psi_{J=1,M=0,j_1=1/2,j_2=3/2,l_1=0,l_2=1} \equiv (1s2p_{3/2}), \quad (83)$$

and examine the positions of the resonances close to $\omega_1^{\rm res} = -E_A + \varepsilon_{1s} + \varepsilon_{2p_{1/2}} + O(\alpha)$ and $\omega_2^{\rm res} = -E_A + \varepsilon_{1s} + \varepsilon_{2p_{3/2}} + O(\alpha)$, respectively.

As has been elaborated in Sec. II the operator V, in general, depends on ω. The position of the resonance can be derived via Taylor expansion at the approximate positions of the resonances $\omega_1^{\rm res} = -E_A + \varepsilon_{1s} + \varepsilon_{2p_{1/2}}$ and $\omega_2^{\rm res} = -E_A + \varepsilon_{1s} + \varepsilon_{2p_{3/2}}$ [see Eq. (65)]. For the practical calculations it is convenient to expand some matrix elements of V at the point $\omega_1^{\rm res}$ and others at the point $\omega_2^{\rm res}$, keeping only terms $O(\alpha^2)$ in both expansions. The resulting inaccuracy can be referred to corrections $O(\alpha^3)$ [24], because at low-Z values the energy difference $\varepsilon_{2p_{1/2}} - \varepsilon_{2p_{3/2}}$ becomes small, while at large-Z values the degeneracy of the levels $2\,^1P_1$ and $2\,^3P_1$ is nearly negligible.

The interelectron interaction correction is represented by the set of graphs (Figs. 7 and 9 which is symmetric under interchange of the upper and lower indices and relabeling of the electrons in the graphs. Accordingly, the operator V is given by a symmetric (and in general complex) matrix. However, as a consequence of performing the Taylor expansion of the matrix elements of V and neglecting third- and higher-orders terms it can lead to a nonsymmetrical matrix. To prevent this asymmetry arising due to purely technical reasons one may symmetrize the matrix V by hand.

Hence, the matrix elements of the frequency-dependent operator V evaluated at the resonances can be written as

$$\langle (1s2p_{1/2})|V(\omega^{\rm res})|(1s2p_{1/2})\rangle = \langle (1s2p_{1/2})|F|(1s2p_{1/2})\rangle, \quad (84)$$

$$\langle (1s2p_{3/2})|V(\omega^{\rm res})|(1s2p_{3/2})\rangle = \langle (1s2p_{3/2})|F|(1s2p_{3/2})\rangle, \quad (85)$$

$$\langle (1s2p_{1/2})|V(\omega^{\rm res})|(1s2p_{3/2})\rangle = \tfrac{1}{2}[\langle (1s2p_{1/2})|F|(1s2p_{3/2})\rangle + \langle (1s2p_{3/2})|F|(1s2p_{1/2})\rangle], \tag{86}$$

$$\langle (1s2p_{3/2})|V(\omega^{\rm res})|(1s2p_{1/2})\rangle = \langle (1s2p_{1/2})|V(\omega^{\rm res})|(1s2p_{3/2})\rangle. \tag{87}$$

The operator F is defined via its action on the set of the one-electron Dirac functions $\{ab\}$, which in our case consists of $\{ab\}=\{1s2p_{1/2}\},\{1s2p_{3/2}\}$. To zeroth-order perturbation theory the operator F reads [see Eq. (72)].

$$F^{(0)}_{a'b'ab} = \varepsilon_a \delta_{a',a} + \varepsilon_b \delta_{b',b}. \tag{88}$$

Being interested in ionization energies it is more convenient to introduce a shifted F with the zeroth-order matrix element

$$F^{(0)}_{a'b'ab} = \varepsilon_a \delta_{a',a} + \varepsilon_b \delta_{b',b} - \varepsilon_{1s} - m, \tag{89}$$

where the electron rest energy m (in relativistic unites) and 1s-electron energy are subtracted. In first-order perturbation theory the interelectron interaction represented by the graph in Fig. 7 can be described by the matrix element

$$F^{(1)}_{a'b'ab} = e^2 I(|\varepsilon_{a'} - \varepsilon_a|)_{a'b'ab}. \tag{90}$$

Since the graph in Fig. 7 is irreducible $F^{(1)}_{a'b'ab}$ coincides with the expression [Eq. (57)] for nondegenerate levels. In second-order perturbation theory we have to account for the two-photon exchange corrections depicted in Fig. 9:

$$F^{(2)(\rm box,irr)}_{a'b'ab} = e^4 \sum_{\rm gg'} \sum_{n_1 n_2} (1 - \delta_{E^{(0)}_{n_1n_2},E^{(0)}_{ab}}) \left\{ \frac{i}{2\pi}\int_{-\infty}^{\infty} d\,\Omega\, \frac{I^{\rm g}(|\,\Omega\,|)_{a'b'n_1n_2} I^{\rm g'}(|\,\Omega - \varepsilon_{a'} + \varepsilon_a|)_{n_1n_2ab}}{(E^{(0)}_{ab} - E^{(0)}_{n_1n_2})(\Omega - \varepsilon_{n_2} + E^{(0)}_{ab} - \varepsilon_{a'} + i0\varepsilon_{n_2})} + \frac{i}{2\pi}\int_{-\infty}^{\infty} d\,\Omega\, \frac{I^{\rm g}(|\,\Omega\,|)_{b'a'n_1n_2} I^{\rm g'}(|\,\Omega - \varepsilon_a + \varepsilon_{a'}|)_{n_1n_2ba}}{(E^{(0)}_{ab} - E^{(0)}_{n_1n_2})(\Omega - \varepsilon_{n_2} + \varepsilon_{a'} + i0\,\varepsilon_{n_2})} \right\}, \tag{91}$$

$$F^{(2)(\rm box,red)}_{a'b'ab} = -\frac{1}{2} e^4 \sum_{\rm gg'} \sum_{n_1n_2} \left\{ \delta_{E^{(0)}_{n_1n_2},E^{(0)}_{ab}} \left[\frac{1}{2\pi}\int_{-\infty}^{\infty} d\,\Omega\, \frac{I^{\rm g}(|\,\Omega\,|)_{a'b'n_1n_2} I^{\rm g'}(|\,\Omega - \varepsilon_{a'} + \varepsilon_a|)_{n_1n_2ab}}{(\Omega - \varepsilon_{n_2} + E^{(0)}_{ab} - \varepsilon_{a'} + i0\varepsilon_{n_2})^2} + \frac{i}{2\pi}\int_{-\infty}^{\infty} d\,\Omega\, \frac{I^{\rm g}(|\,\Omega\,|)_{b'a'n_1n_2} I^{\rm g'}(|\,\Omega - \varepsilon_a + \varepsilon_{a'}|)_{n_1n_2ba}}{(\Omega - \varepsilon_{n_2} + \varepsilon_{a'} + i0\,\varepsilon_{n_2})^2} \right] + \delta_{E^{(0)}_{n_1n_2},E^{(0)}_{a'b'}} (1 - \delta_{E^{(0)}_{n_1n_2},E^{(0)}_{ab}}) \times \left[\frac{I(|\varepsilon_{n_2} - E^{(0)}_{ab} + \varepsilon_{a'}|)_{a'b'n_1n_2} I(|\varepsilon_{n_2} - E^{(0)}_{ab} + \varepsilon_a|)_{n_1n_2ab}}{E^{(0)}_{ab} - E^{(0)}_{n_1n_2}} + \frac{I(|\varepsilon_{n_2} - \varepsilon_{a'}|)_{b'a'n_1n_2} I(|\varepsilon_{n_2} - \varepsilon_a|)_{n_1n_2ba}}{E^{(0)}_{ab} - E^{(0)}_{n_1n_2}} \right] \right\}, \tag{92}$$

$$F^{(2)(\rm cross,irr)}_{a'b'ab} = e^4 \sum_{\rm gg'} \sum_{n_1n_2} \left\{ (1 - \delta_{0,(\varepsilon_{n_2} - \varepsilon_{n_1} + \varepsilon_b - \varepsilon_{a'})}) \frac{i}{2\pi}\int_{-\infty}^{\infty} d\,\Omega\, \frac{I^{\rm g}(|\,\Omega\,|)_{b'n_2n_1a} I^{\rm g'}(|\,\Omega - \varepsilon_{a'} + \varepsilon_a|)_{n_1a'bn_2}}{(\varepsilon_{n_2} - \varepsilon_{n_1} + \varepsilon_b - \varepsilon_{a'})(\Omega - \varepsilon_{n_2} + \varepsilon_a + i0\varepsilon_{n_2})} + (1 - \delta_{0,(\varepsilon_{n_2} - \varepsilon_{n_1} - \varepsilon_b + \varepsilon_{a'})}) \frac{i}{2\pi}\int_{-\infty}^{\infty} d\,\Omega\, \frac{I^{\rm g}(|\,\Omega\,|)_{n_1b'an_2} I^{\rm g'}(|\,\Omega - \varepsilon_{a'} + \varepsilon_a|)_{a'n_2n_1b}}{(\varepsilon_{n_2} - \varepsilon_{n_1} - \varepsilon_b + \varepsilon_{a'})(\Omega - \varepsilon_{n_2} + E^{(0)}_{ab} - \varepsilon_{a'} + i0\varepsilon_{n_2})} \right\}, \tag{93}$$

$$F^{(2)(\rm cross,red)}_{a'b'ab} = e^4 \sum_{\rm gg'} \sum_{n_1n_2} \delta_{0,(\varepsilon_{n_2} - \varepsilon_{n_1} + \varepsilon_b - \varepsilon_{a'})} \frac{i}{2\pi}\int_{-\infty}^{\infty} d\,\Omega \times \frac{I^{\rm g}(|\,\Omega\,|)_{b'n_2n_1a} I^{\rm g'}(|\,\Omega - \varepsilon_{a'} + \varepsilon_a|)_{n_1a'bn_2}}{(\Omega - \varepsilon_{n_2} + \varepsilon_a + i0\,\varepsilon_{n_2})^2}. \tag{94}$$

In Eqs. (91) and (92) the notations $E^{(0)}_{ab}=\varepsilon_a+\varepsilon_b$, $E^{(0)}_{a'b'}=\varepsilon_{a'}+\varepsilon_{b'}$, and $E^{(0)}_{n_1n_2}=\varepsilon_{n_1}+\varepsilon_{n_2}$ are introduced. The index g runs over c,t (scalar and transverse photons). The Kronecker symbols ensure that terms with potentially zero denominators will be omitted in the summation over n_1, n_2.

Note that Eqs. (91), (93), and (94) for the irreducible parts coincide generically with Eq. (58) for nondegenerate levels (see also [13]). However, for the reducible part of the "box" graph additional terms originating from the geometric progression for the one-photon exchange graph (nondiagonal matrix elements of the second term of the progression) occur.

TABLE I. Matrix elements of the operator V for the two-electron configurations $2\,^1P_1$ and $2\,^3P_1$ (eV). The individual contributions for the Dirac-binding energies of $2p$-electron states ($V^{(0)}$), the one-photon exchange contribution ($V^{(1)}$), and the two-photon contribution ($V^{(2)}$) are compiled, respectively. $E_X(2\,^1P_1)$ and $E_X(2\,^3P_1)$ are the energies of the corresponding configurations, where only the photon exchange contributions are taken into account (neglecting radiative corrections).

Contribution	$Z=10$	18	26	30	40
$(1s2p_{1/2}),(1s2p_{1/2})$	−340.7099	−1108.0574	−2325.7285	−3108.3193	−5594.0369
$V^{(0)}$: $(1s2p_{3/2}),(1s2p_{3/2})$	−340.2556	−1103.2520	−2304.5586	−3070.5057	−5471.5704
$(1s2p_{1/2}),(1s2p_{3/2})$	0	0	0	0	0
$(1s2p_{1/2}),(1s2p_{1/2})$	$64.7130+0.0007i$	$117.2696+0.0072i$	$171.2105+0.0316i$	$198.9154+0.0560i$	$271.1021+0.1778i$
$V^{(1)}$: $(1s2p_{3/2}),(1s2p_{3/2})$	$67.6938-0.0007i$	$122.1610-0.0072i$	$177.1674-0.0312i$	$204.9502-0.0551i$	$275.4795-0.1724i$
$(1s2p_{1/2}),(1s2p_{3/2})$	$4.3418-0.0019i$	$7.6653-0.0204i$	$10.7333-0.0887i$	$12.1369-0.1571i$	$15.1577-0.4954i$
$(1s2p_{1/2}),(1s2p_{1/2})$	−2.7692	−2.8168	−2.8938	−2.9439	−3.1082
$V^{(2)}$: $(1s2p_{3/2}),(1s2p_{3/2})$	−3.5256	−3.5603	−3.6142	−3.6506	−3.7641
$(1s2p_{1/2}),(1s2p_{3/2})$	−1.0727	−1.0618	−1.0450	−1.0350	−1.0008
$E_X(2\,^1P_1)$	−273.8939	−981.1501	−2127.8323	−2866.5171	−5198.2878
$E_X(2\,^3P_1)$	−280.9596	−997.1059	−2160.5849	−2915.0368	−5327.6102
$\Delta E_X(2\,^1P_1)$: Appr. 1	2.1934	3.5012	3.1731	2.6890	1.5672
$\Delta E_X(2\,^3P_1)$: Appr. 1	−2.1934	−3.5012	−3.1731	−2.6890	−1.5672
$\Delta E_X(2\,^1P_1)$: Appr. 2	−0.7581	−0.7203	−0.5599	−0.4460	−0.2175
$\Delta E_X(2\,^3P_1)$: Appr. 2	0.7581	0.7203	0.5599	0.4460	0.2175
$\Delta E_X(2\,^1P_1)$: Appr. 3	0.0001	0.0019	0.0102	0.0168	0.0571
$\Delta E_X(2\,^3P_1)$: Appr. 3	0.0000	−0.0009	−0.0036	−0.0056	−0.0121
$\Delta E_X(2\,^1P_1)$: Appr. 4	0.0000	0.0002	0.0009	−0.0005	−0.0013
$\Delta E_X(2\,^3P_1)$: Appr. 4	0.0000	0.0000	0.0009	0.0018	0.0038
$\Delta E_X(2\,^1P_1)$: Appr. 5	0.0000	0.0000	−0.0001	−0.0003	−0.0015
$\Delta E_X(2\,^3P_1)$: Appr. 5	0.0000	0.0000	0.0001	0.0003	0.0015
$\Delta E_X(2\,^1P_1)-E_X(2\,^3P_1)$					
This work	7.0657	15.9557			
Lindgren *et al.* [28]	7.0657	15.9554			

Contribution	$Z=50$	60	70	80	92
$(1s2p_{1/2}),(1s2p_{1/2})$	−8884.368	−13062.966	−18250.182	−24621.409	−34211.065
$V^{(0)}$: $(1s2p_{3/2}),(1s2p_{3/2})$	−8575.514	−12395.463	−16948.025	−22253.673	−29649.834
$(1s2p_{1/2}),(1s2p_{3/2})$	0	0	0	0	0
$(1s2p_{1/2}),(1s2p_{1/2})$	$348.917+0.437i$	$434.638+0.912i$	$531.400+1.702i$	$643.793+2.930i$	$809.699+5.178i$
$V^{(1)}$: $(1s2p_{3/2}),(1s2p_{3/2})$	$347.960-0.415i$	$422.949-0.846i$	$501.042-1.531i$	$582.883-2.533i$	$686.996-4.210i$
$(1s2p_{1/2}),(1s2p_{3/2})$	$17.320-1.206i$	$18.430-2.491i$	$18.311-4.590i$	$16.795-7.777i$	$12.929-13.440i$
$(1s2p_{1/2}),(1s2p_{1/2})$	−3.333	−3.635	−4.038	−4.585	−5.531
$V^{(2)}$: $(1s2p_{3/2}),(1s2p_{3/2})$	−3.915	−4.105	−4.339	−4.628	−5.053
$(1s2p_{1/2}),(1s2p_{3/2})$	−0.955	−0.893	−0.801	−0.771	−0.683
$E_X(2\,^1P_1)$	−8230.604	−11976.160	−16451.098	−21675.333	−28967.898
$E_X(2\,^3P_1)$	−8539.649	−12632.423	−17723.044	−23982.287	−33406.890
$\Delta E_X(2\,^1P_1)$: Appr. 1	0.865	0.460	0.225	0.085	−0.007
$\Delta E_X(2\,^3P_1)$: Appr. 1	−0.865	−0.460	−0.225	−0.085	0.007
$\Delta E_X(2\,^1P_1)$: Appr. 2	−0.102	−0.049	−0.023	−0.011	−0.004
$\Delta E_X(2\,^3P_1)$: Appr. 2	0.102	0.049	0.023	0.011	0.004
$\Delta E_X(2\,^1P_1)$: Appr. 3	0.153	0.358	0.759	1.461	2.931
$\Delta E_X(2\,^3P_1)$: Appr. 3	−0.014	−0.007	0.021	0.096	0.323
$\Delta E_X(2\,^1P_1)$: Appr. 4	−0.004	−0.009	−0.015	−0.035	−0.075
$\Delta E_X(2\,^3P_1)$: Appr. 4	0.011	0.025	0.050	0.094	0.181
$\Delta E_X(2\,^1P_1)$: Appr. 5	−0.004	−0.009	−0.016	−0.026	−0.041
$\Delta E_X(2\,^3P_1)$: Appr. 5	0.004	0.009	0.016	0.026	0.041

It is easy to make sure that the contribution of reference states ($E^{(0)}_{n_1n_2}=E^{(0)}_{ab}, E^{(0)}_{n_1n_2}=E^{(0)}_{a'b'}$) to the exchange of two Coulomb photons (or Breit photons with neglect of retardation) is absent.

IV. NUMERICAL RESULTS AND THEIR ANALYSIS

The results of the numerical calculations are presented in Tables I and II. To account for nuclear size corrections we solved the Dirac equation with the Coulomb potential generated by a nuclear charge density described by a Fermi distribution. The parameters of the Fermi distribution are taken from Ref. [13].

In Table I we present a detailed analysis of our results obtained for the photon exchange contribution. The value $V^{(0)}$ is the binding energy of the $2p$ state according to Eq. (89), the value $V^{(1)}$ corresponds to the one-photon exchange contribution Eq. (90), and $V^{(2)}$ represents the two-photon exchange contributions given by Eqs. (91)–(94). We note that, in general, the matrix V has complex elements and both their real and imaginary parts contribute to the energy eigenvalues—i.e., the real part of the diagonalized matrix V. In our calculation the imaginary part of $V^{(1)}$ is taken into account, while the imaginary part of the two-photon exchange contribution ($V^{(2)}$) is neglected. The values $E_{\mathrm{X}}(2^1P_1)$ and $E_{\mathrm{X}}(2^3P_1)$ denote the photon-exchange contribution to the energies of the corresponding electron configurations (neglecting the radiative corrections). For $Z=10,18$ we present also the values for the difference between the energies of the levels under consideration reported in Ref. [28].

In order to analyze the influence of the quasidegeneracy on QED effects in more detail we compile the corresponding energy shifts of the levels due to the photon exchange contribution calculated within various approximations. The differences between the energies of the levels calculated without the approximations and the energies calculated within the framework of the approximations are presented in Table I [$\Delta E_{\mathrm{X}}(2^{1,3}P_1)$: Appr. 1–5].

Approximation 1: We omit the nondiagonal elements of the matrix $V=V^{(0)}+V^{(1)}+V^{(2)}$. Consequently, effects of the quasidegeneracy are totally neglected.

Approximation 2: We omit the nondiagonal elements only in the matrix $V^{(2)}$. As stated above the expression for the one-photon exchange correction Eq (90), does not depend on ω and coincides with the one for the nondegenerate case. Accordingly, the first-order contribution is taken into account just as the solution of the secular equation—i.e., following the usual techniques developed in quantum mechanics for treating degenerate levels. The influence of quasidegeneracy due to the second-order matrix element $V^{(2)}$ is neglected.

Approximation 3: We calculate the matrix elements of V within the framework of RMBPT. Compared with the full *ab initio* QED calculation the following contributions are missing: (1) negative-energy intermediate states, (2) crossed-photon interaction, and (3) rigorous treatment of retardation effects. As mentioned above within the framework of RMBPT no contribution due to reference states (for two-photon exchange) arises. Accordingly, the energies of the levels just follow as solutions of the secular equation.

Approximation 4: Only the matrix elements of $V^{(2)}$ are evaluated within the framework of RMBPT. According to the comment made on approximation 2, this also follows the quantum-mechanical treatment for quasidegeneracy.

Approximation 5: We neglect the imaginary part of the elements of the matrix V. The matrix V defined in Eq. (73) is a complex one. Although the energy of the level is defined as the real part of the diagonalized matrix $V(\omega)$ at the point of the resonance ($\omega=\omega^{\mathrm{res}}$), the imaginary part of the elements of the matrix V (nondiagonal) contributes to the energy.

TABLE II. Data for the energies (in eV) of the configurations $2\,^1P_1$ and $2\,^3P_1$. Photon exchange corrections are taken into account up to second order in α. Self-energy (SE) and vacuum-polarization (VP) corrections are taken into account only in first order. The one-electron radiative corrections of order α^2, the SE and VP screening corrections, and all the corrections of the third and higher orders are omitted. The data are compared with the results of Plante *et al.* [2] and Drake [1].

Contribution	$Z=10$	18	26	30	40
$E(2^1P_1)$, this work	−273.8936	−981.1462	−2127.8070	−2866.4666	−5198.0971
$E(2^3P_1)$, this work	−280.9596	−997.1079	−2160.5953	−2915.0545	−5327.6408
$E(2^1P_1)$, Plante *et al.*	−273.8155	−981.0966	−2127.7712	−2866.4354	−5198.0801
$E(2^3P_1)$, Plante *et al.*	−281.0132	−997.1451	−2160.6313	−2915.0924	−5327.6917
$E(2^1P_1)$, Drake	−273.8077	−981.0832	−2127.7515	−2866.4129	−5198.0515
$E(2^3P_1)$, Drake	−281.0054	−997.1303	−2160.6038	−2915.0556	−5327.6222
Contribution	$Z=50$	60	70	80	92
$E(2^1P_1)$, this work	−8230.079	−11974.951	−16448.629	−21670.722	−28958.974
$E(2^3P_1)$, this work	−8539.626	−12632.120	−17721.892	−23979.001	−33397.135
$E(2^1P_1)$, Plante *et al.*	−8230.078	−11974.972	−16448.682	−21670.812	−28959.135
$E(2^3P_1)$, Plante *et al.*	−8539.719	−12632.321	−17722.363	−23980.133	−33400.643
$E(2^1P_1)$, Drake	−8230.038	−11974.910	−16448.591	−21670.679	−28958.944
$E(2^3P_1)$, Drake	−8539.592	−12632.088	−17721.944	−23979.373	−33398.993

TABLE III. Theoretical and experimental data for $2\,^3P_1-2\,^1P_1$ transition energies (in eV).

Z	This work	Lindgren *et al.* [28]	Plante *et al.* [2]	Drake [1]	Experiment	Ref.
18	15.9617	16.0550	16.0485	16.0471	16.031(0.074)	[43]
					16.00(0.49)	[44]
26	32.7883		32.8601	32.8523	33.4(0.5)	[45]
					33.23(0.45)	[46,45]
92	4438.161		4441.508	4440.049	4455.(87.)	[47]

The results in Table I demonstrate that for the $2\,^1P_1$, and $2\,^3P_1$ levels a complete *ab initio* QED theory for describing the quasidegeneracy has to be employed only when going beyond the level of second-order corrections. For $Z<30$ approximation 3 provides an accuracy of about 1% at the level of second-order perturbation theory. Accordingly, the inaccuracy can be referred to corrections of third order. For $Z<60$—70 approximation 4 leads to an inaccuracy comparable in magnitude with the corrections of third order. For $Z>60$—70 the effect of quasidegeneracy decreases definitely to the level of third-order corrections. Consequently, approximation 2 can be employed for high-Z systems. For $Z>80$ the quasidegeneracy becomes completely negligible i.e., it will be sufficient to employ approximation 1. The contribution of imaginary parts of the matrix elements V to the energy levels appears as an effect of quasidegeneracy, which originates completely from QED. It is perceptible only for high $Z>70$, which also reveals that the neglect of the imaginary part of $V^{(2)}$ has been legitimate.

In Table II we present the data for the total energies of the $2\,^1P_1$ and $2\,^3P_1$ two-electron configurations, respectively. The numbers present the ionization energy of the $2p$-electron with the opposite sign. These data are compared with the results obtained by Plante *et al.* [2] and Drake [1]. Two different approximate methods have been employed in these works: the "relativistic AO theory" [2] and "the unified theory" [1]. The latter methods account approximately for QED effects, such as retardation, crossed-photon graphs, and negative-energy intermediate states, while taking into account partially higher orders of the perturbation theory. In the present work the photon exchange is taken into account up to second order. The SE and VP corrections are included only in first order. Quantitative results for SE and VP corrections are taken from Refs. [40–42,3]. The SE and VP screening corrections, the radiative corrections of second order, and all the corrections of third and higher orders are omitted. We note that the VP screening corrections for the states considered have been evaluated by Artemyev *et al.* [15], while results for the SE screening corrections are not yet available. Since the SE and VP screening corrections partially cancel each other, we do not include the results of [15] in Table II. In Table III we present various theoretical and experimental data for $2\,^3P_1-2\,^1P_1$ transition energies. We conclude that the discrepancy between our data and those from other results arising for small values of Z is caused by third and higher orders of the perturbation theory which have not been accounted for in the present paper. For high Z the major inaccuracy is due to missing self-energy, vacuum-polarization screening corrections, and one-electron radiative corrections of second order.

ACKNOWLEDGMENTS

The authors are indebted to Professor W. Nagel from the center of high-performance computing at TU Dresden for providing access to all necessary computer facilities. O.Y.A. is grateful to TU Dresden for the hospitality during his visits in 2002 and 2003 and to the DFG for financial support. The work of O.Y.A. and L.N.L. was supported by RFBR Grant No. 02-02-16578 and by Minobrazovanie Grant No. E02-3.1-7. G.P. and G.S. acknowledge financial support from BMBF, DFG, and GSI.

[1] G. W. Drake, Can. J. Phys. **66**, 586 (1988).
[2] D. R. Plante, W. R. Johnson, and J. Sapirstein, Phys. Rev. A **49**, 3519 (1994).
[3] P. J. Mohr, G. Plunien, and G. Soff, Phys. Rep. **293**, 227 (1998).
[4] V. A. Yerokhin, P. Indelicato, and V. M. Shabaev, Phys. Rev. Lett. **91**, 073001 (2003).
[5] G. L. Klimchitskaya and L. N. Labzowsky, Zh. Eksp. Teor. Fiz. **60**, 2019 (1971) [Sov. Phys. JETP **33**, 1088 (1971)].
[6] L. Labzowsky, G. Klimchitskaya, and Yu. Dmitriev, *Relativistic Effects in the Spectra of Atomic Systems* (Institute of Physics Publishing, Bristol, 1993).
[7] S. Blundell, P. J. Mohr, W. R. Johnson, and J. Sapirstein, Phys. Rev. A **48**, 2615 (1993).
[8] I. Lindgren, H. Persson, S. Salomonson, and L. Labzowsky, Phys. Rev. A **51**, 1167 (1995).
[9] V. A. Yerokhin, A. N. Artemyev, V. M. Shabaev, M. M. Sysak, O. M. Zherebtsov, and G. Soff, Phys. Rev. Lett. **85**, 4699 (2000).
[10] P. J. Mohr and J. Sapirstein, Phys. Rev. A **62**, 052501 (2000).
[11] O. Yu. Andreev, L. N. Labzowsky, G. Plunien, and G. Soff, Phys. Rev. A **64**, 042513 (2001).
[12] B. Åsén, S. Salomonson, and I. Lindgren, Phys. Rev. A **65**, 032516 (2002).
[13] O. Yu. Andreev, L. N. Labzowsky, G. Plunien, and G. Soff, Phys. Rev. A **67**, 012503 (2003).

[14] P. Indelicato and P. J. Mohr, Phys. Rev. A **63**, 052507 (2001).
[15] A. N. Artemyev, T. Beier, G. Plunien, V. M. Shabaev, G. Soff, and V. A. Yerokhin, Phys. Rev. A **62**, 022116 (2000).
[16] V. A. Yerokhin, A. N. Artemyev, T. Beier, G. Plunien, V. M. Shabaev, and G. Soff, Phys. Rev. A **60**, 3522 (1999).
[17] A. N. Artemyev, T. Beier, G. Plunien, V. M. Shabaev, G. Soff, and V. A. Yerokhin, Phys. Rev. A **60**, 45 (1999).
[18] M. Gell-Mann and F. Low, Phys. Rev. **84**, 350 (1951).
[19] J. Sucher, Phys. Rev. **107**, 1448 (1957).
[20] L. N. Labzowsky, Zh. Eksp. Teor. Fiz. **59**, 167 (1970) [Sov. Phys. JETP **32**, 94 (1970)].
[21] M. Braun and V. Shirokov, Izv. Akad. Nauk SSSR, Ser. Fiz. **41**, 2585 (1977) [Bull. Acad. Sci. USSR, Phys. Ser. (Engl. Transl.) **41**, 2585 (1977)].
[22] V. M. Shabaev, Teor. Mat. Fiz. **82**, 83 (1990) [Theor. Math. Phys. **82**, 57 (1990)].
[23] V. M. Shabaev, J. Phys. B **26**, 4703 (1993).
[24] V. M. Shabaev, Phys. Rep. **356**, 119 (2002).
[25] L. Labzowsky, V. Karasiev, I. Lindgren, H. Persson, and S. Salomonson, Phys. Scr. **T46**, 150 (1993).
[26] L. N. Labzowsky, A. Prosorov, A. V. Shonin, I. Bednyakov, G. Plunien, and G. Soff, Ann. Phys. (N.Y.) **302**, 22 (2002).
[27] É.-O. Le Bigot, P. Indelicato, and V. M. Shabaev, Phys. Rev. A **63**, 040501 (2001).
[28] I. Lindgren, B. Åsén, S. Salomonson, and A.-M. Mårtensson-Pendrill, Phys. Rev. A **64**, 062505 (2001).
[29] V. Weisskopf and E. Wigner, Z. Phys. **63**, 54 (1930).
[30] F. Low, Phys. Rev. **88**, 53 (1952).
[31] L. N. Labzowsky, Zh. Eksp. Teor. Fiz. **85**, 869 (1983) [Sov. Phys. JETP **58**, 503 (1983)].
[32] L. N. Labzowsky, J. Phys. B **26**, 1039 (1993).
[33] V. G. Gorshkov, L. N. Labzowsky, and A. A. Sultanaev, Zh. Eksp. Teor. Fiz. **96**, 53 (1989) [Sov. Phys. JETP **69**, 28 (1989)].
[34] V. V. Karasiev, L. N. Labzowsky, A. V. Nefiodov, V. G. Gorshkov, and A. A. Sultanaev, Phys. Scr. **46**, 225 (1992).
[35] L. Labzowsky, V. Karasiev, and I. Goidenko, J. Phys. B **27**, L439 (1994).
[36] L. N. Labzowsky, I. A. Goidenko, and D. Liesen, Phys. Scr. **56**, 271 (1997).
[37] L. N. Labzowsky and M. A. Tokman, Adv. Quantum Chem. **30**, 393 (1998).
[38] L. N. Labzowsky and A. O. Mitrushenkov, Phys. Rev. A **53**, 3029 (1996).
[39] L. N. Labzowsky, *Teoriya atoma: Kvantovaya elektrodinamika elektronnyh obolochek i processy izlucheniya [Theory of atoms: Quantum electrodynamics of the electron shells and the processes of radiation]* (Nauka, Moscow, 1996) (in Russian).
[40] P. J. Mohr, Phys. Rev. A **46**, 4421 (1992).
[41] P. J. Mohr and G. Soff, Phys. Rev. Lett. **70**, 158 (1993).
[42] G. Soff and P. J. Mohr, Phys. Rev. A **38**, 5066 (1988).
[43] R. D. Deslattes, H. F. Beyer, and F. Folkmann, J. Phys. B **17**, L689 (1984).
[44] J. P. Briand, J. P. Mossé, P. Indelicato, P. Chevallier, D. Girard-Vernhet, A. Chetioui, M. T. Ramos, and J. P. Desclaux, Phys. Rev. A **28**, 1413 (1983).
[45] J. P. Briand, M. Tavernier, R. Marrus, and J. P. Desclaux, Phys. Rev. A **29**, 3143 (1984).
[46] P. Beiersdorfer, M. Bitter, S. von Goeler, and K. W. Hill, Phys. Rev. A **40**, 150 (1989).
[47] J. P. Briand, P. Chevallier, P. Indelicato, K. P. Ziock, and D. D. Dietrich, Phys. Rev. Lett. **65**, 2761 (1990).